AD-A071 418 MARYLAND UNIV COLLEGE PARK DEPT OF AEROSPACE ENGINEERING F/G 20/4
NEW COMPUTATIONAL MODELS IN CONTINUUM MECHANICS.(U)
MAR 79 O BELOTSERKOVSKII N00014-79-M-0022
UNCLASSIFIED AE-79-1 NL

END
DATE FILMED
8-79
DDC

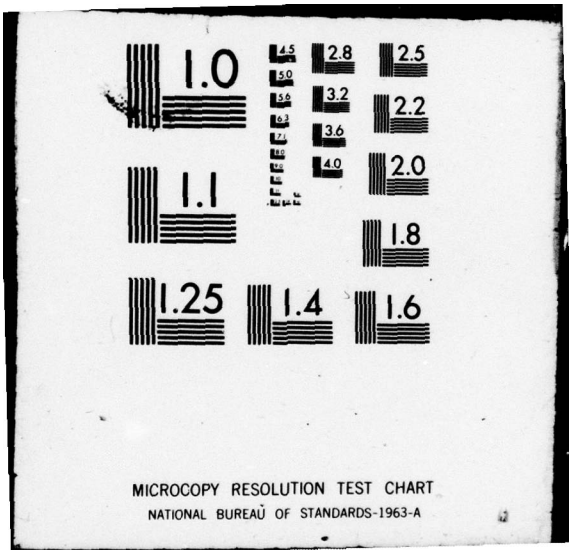
1.0
1.1
1.25
1.4
1.6
1.8
2.0
2.2
2.5
2.8
3.2
3.6
4.0
4.5
5.0
5.6
6.3
7.1
MICROCOPY RESOLUTION TEST CHART
NATIONAL BUREAU OF STANDARDS-1963-A

Technical Report No. AE-79-1

(12) LEVEL II

University of Maryland, College Park
Department of Aerospace Engineering

NEW COMPUTATIONAL MODELS IN CONTINUUM MECHANICS

by

PROF. OLEG BELOTSERKOVSKII
Computing Center
Academy of Sciences of the USSR

Office of Naval Research
Fluid Dynamics Program
Arlington, Virginia 22217

Contract N00014-79-M-0022
NR 061-262
MARCH, 1979

(14) Technical Report No. AE-79-1

UNIVERSITY OF MARYLAND, COLLEGE PARK
DEPARTMENT OF AEROSPACE ENGINEERING

(6) # NEW COMPUTATIONAL MODELS IN CONTINUUM MECHANICS

by

(10) PROFESSOR OLEG BELOTSERKOVSKII
Computing Center
Academy of Sciences of the USSR

(9) Final technical rept.,

Office of Naval Research
Fluid Dynamics Program
Arlington, Virginia 22217

(15) Contract N00014-79-M-0022
NR 061-262

(11) Mar[redacted]79

(12) 94p.

401 860

NEW COMPUTATIONAL MODELS IN CONTINUUM MECHANICS

O.M. Belotserkovskii *

Direct numerical simulation of complex gas dynamics problems (computational experiment) is performed with the help of Euler, Navier-Stokes and Boltzmann equations. The basic principles of the computational experiment are formulated and the results for various gas dynamics problems of a complex internal structure are presented.

The problems examined include the transonic regime (super-critical flows including transition through sound velocity), flows with a jet "injected" into the main stream and diffraction problems. Body wake flows are studied at various Reynolds numbers. The structure of a shock wave provides an example of rarefied gas flows at various Mach numbers.

A set of control tests is worked out for the estimation of calculation accuracy.

* Professor, Member of the Academy of Sciences of the USSR, Computing Center, Academy of Sciences, 40 Vavilova St., Moscow V-333, U.S.S.R.

Preface

Selected results of this report and its companion, "Investigation of Transonic Gas Flows," were communicated in seminar lectures given by Prof. Belotserkovskii at several American universities during a 4-week visit in November - December, 1978. His lecture on "New Computational Models in Continuum Mechanics," presented December 1, 1978, at a seminar of the Aerospace Engineering Department of the University of Maryland at College Park, attracted considerable interest from a diverse audience of scientists and engineers. In response to numerous requests Prof. Belotserkovskii made available the manuscripts of two reports which describe in some detail the computational techniques employed in the numerical solutions of the problems surveyed in his seminar talks.

This report is a survey of computational models developed by the author in collaboration with his colleagues at the Computational Center of the USSR Academy of Sciences over the past decade. Although most of these results have previously appeared in various Soviet journals, with the most recent contribution, the last chapter of the present report, in the proceedings of the VI International Conference of Computational Methods of Hydrodynamics, Vol. 2, Moscow, 1978, pp. 37-47, this report nevertheless gives a coherent review of the advances in computational fluid dynamics at one of the foremost centers of the Soviet Union.

The hallmarks of their numerical techniques are that they are:

(1) typically differentially and globally conservative, and

(2) careful attention is made to minimize truncation errors while at the same time the favorable properties of the computational schemes are exploited, e.g., the effective viscosity of the

finite-difference equations (to promote calculational stability) and (physically interpretted) the ability to compute the essential features of separated regions of recirculating flows (e.g., wakes) wholey within the framework of the Euler equations.

The underlying theme of this work is perhaps best described by the author. "The properties that a numerical method is to be endowed with, from the view-point of modern developments, are so diverse that they are difficult to fully implement in one single method. In view of this, complexes of numerical methods based upon a unified approach should be available. Finally, it is desirable to consider homogeneous schemes that enable calculations through discontinuities that may arise in the evolution of the solution, that allow for explicitly singling out some (principal) of the features and that adequately resolve their boundary conditions."

The numerical methods are illustrated by a great variety of computational results which encompass a wide range of velocities, from subsonic through transonic as well as up to hypersonic wherein complex physical processes (thermo-chemical and radiation) strongly affect the resulting flow field and over a wide range of Reynold's numbers in the case of viscous compressible gas flows. Wherever possible English translations of the references have been cited.

The careful typing of the edited manuscript by Miss Vicki Brewer deserves a special note of appreciation. Finally, I am pleased to acknowledge Contract N0014-79-M-0022 from the U.S. Office of Naval Research which made possible the publication and distribution of this report.

W. L. Melnik, Editor
Professor, Aerospace Engineering Dept.
University of Maryland at College Park

TABLE OF CONTENTS

LIST OF FIGURES

1. Introduction

At present, specialists of applied sciences are confronted with various kinds of practical problems whose successful and accurate solution, in most cases, may be obtained only by numerical methods with the aid of computers. However, this does not mean that analytical methods which enable us to find the solution in "closed" form will not be developed. Nevertheless, it is absolutely clear that the range of problems permitting such an approach to their solution is rather narrow, therefore, the development of general numerical algorithms for the investigation of problems of mathematical physics (gas dynamics, theory of elasticity, etc.) is especially important.

a) Difficulties of Carrying Out the Experiment.

At hypersonic flight velocities, the resulting high temperatures give rise to effects of dissociation and ionization in the flow and, in a number of cases, even to "luminescence" of the gas. In these cases it is enormously difficult to simulate the experiment in the laboratory, since it is not sufficient to satisfy the classical criteria of similarity, i.e., the equality of the Mach and Reynolds numbers. The equality of absolute pressures and absolute temperatures is also required, which is only possible if the sizes of the model and prototype are identical. These requirements pose numerous technical difficulties and not the least of which concerns the high cost of the experiment.

However, the importance of the experiment must not be underestimated for it is always the basis of measure for confirming (or rejecting) the calculation scheme and numerical solution.

b) Complexity of the Equations Considered.

The prominance of numerical methods in mechanics of continua is partly explained by the fact that the governing equations of aerodynamics and gas dynamics, and of theory of elasticity represent the most complicated (as compared to other branches of mathematics) system of partial differential equations. In the general case, this is a nonlinear system of mixed type (wherein the surface across which the equations change their type is unspecified) and with "movable boundaries", i.e., the boundary conditions are given on surfaces or lines which, in turn, are determined by the calculations. Moreover, the range of the unknown functions is so wide that ordinary methods of analytical investigation (linearization of equations, series expansion, separation of a small parameter, etc.) are not appropriate for the development of the complete solution of the problem in the general case.

It should be noted, that in solving complicated problems on electronic computers that the preliminary analytical investigation of a problem may provide great insight and sometimes this investigation is simply decisive for the successful realization of the numerical algorithm.

Let us dwell on one more peculiarity of algorithms used for solving concrete problems of mechanics of continua. Currently, numerical methods have found a wide practical application in design offices and research institutes. Substantial progress in the exploration of the cosmos, in the optimum control of vehicles, in the choice of rational configurations of vehicles and etc., are, to a considerable extent, due to scientific information obtained from serial calculations. The volume of information obtained by means of the calculation is far more complete and substantially

cheaper than the corresponding experimental investigations if the problem is correctly formulated, well simulated and algorithmically rational. However, a wide application of the numerical methods for practical purposes requires sufficient simplicity and reliability. Thus, on the one hand, one has to deal with rather complicated mathematical problems, while on the other hand, it is necessary to develop rather simple and reliable numerical methods permitting us to carry out serial calculations at project institutes and design offices.

Note that for most problems in gas dynamics, not only have no mathematical theorems of existence and uniqueness been proved, but very often there is no confidence that such theorems can even be derived. As a rule, the very mathematical formulation of the problem is not strictly given and only the physical treatment is presented, which is far from being one and the same thing. The mathematical difficulties of the investigation of such types of problems are related to the nonlinearity of the equations, as well as to the number of independent variables.

The state of affairs with the methods of solution are no better. So far, investigations related to the possibility of realization of the algorithm, its convergence to the unknown solution, and its stability have rigorously been preformed only for linear systems, and, in a number of cases, only for equations with constant coefficients. When confronted with the necessity of solving a problem, the mathematician often has to use the known algorithms and to develop new methods without a rigorous mathematical basis for their applicability.

In science, as well as in mathematics, one can find many examples when new ideas and concepts were successfully used without

a rigorous basis which only appeared later. Of course, this does not suggest, that when developing new numerical algorithms, one may slight the accurate formulation of the problem or its physical meaning. This oversight inevitably leads to numerous mistakes, consequently a waste of time and, moreover, the experience without being theoretically interpreted does not give the foundation for further development of the method.

We want to draw your attention to this rather clear question only because there is still prevalent an opinion, that the main thing is to write down differential equations and all the rest reduces to a trivial substitution of derivatives by differences and to programming on which too much importance is sometimes attached. In this connection, it is reasonable to formulate the main stages of the numerical solution to a physical problem with the aid of computers in the following way:

1) the construction of a physical model and the mathematical statement of the problem;

2) the development of a numerical algorithm and its theoretical interpretation;

3) programming (manual or automatic) and the formal adjustment of the program;

4) the methodical adjustment of the algorithm, i.e., the test of its operation by concrete problems; the elimination of drawbacks uncovered and the experimental investigation of the algorithm;

5) accumulation of experience, the estimation of effectiveness and the range of applicability of the algorithm from serial calculations.

At all stages, the mathematical theory, the physical and computational experiment are used jointly and consistently. Their application may be

illustrated by solving concrete problems, which will be described below. Therefore, we shall make only some common observations by way of introduction.

The main principle of using mathematical results is that the conditions providing the solution of a problem for special simplified cases must be fulfilled as well for more general cases. Parallel to this, consideration of the physical phenomenon provides a qualitative picture against which the statement of the problem is checked and defined more exactly. Ultimately, the final experimental test allows us to access the correctness of the assumptions made and the validity of the algorithm and resulting solution. It should be noted, that the estimate of accuracy of the numerical solution must be done purely mathematically, without using the results of the physical experiment. The latter may be used for qualitative comparison while the quantitative comparison between the calculation and experiment provides information on how closely the physical model used approaches the natural environment.

1.1 Numerical Methods of Solution of Equations of Gasdynamics.

Many important problems of the exact sciences involve the solution of a system of non-linear partial differential equations. Oftentimes it includes many problems with discontinuous solutions (e.g., gas dynamics).

The construction of reasonably accurate solutions of the exact equations of gasdynamics in the general case has become possible only with the aid of numerical methods, exploiting the advantages of high-speed electronic digital computing machines. Technological requirements have called for an intensive development of numerical methods and their application to the solution of a wide variety of gas dynamics problems. Scientists and

research engineers in the area of gas dynamics have contributed significantly to the development of modern numerical methods of solving systems of non-linear partial differential equations.

There exist four universal numerical methods which are applicable to the solution of non-linear partial differential equations of gas dynamics problems.

I. Method of Finite Differences. This method is the most highly developed of the four at the present time and is widely applied to the solution of both linear and non-linear equations of the hyperbolic, elliptic and parabolic types. The region of integration is subdivided into a network of computational cells by a generally fixed orthogonal mesh. Derivatives of functions in the various directions are replaced by finite differences of one form or another; usually, a so-called implicit difference scheme is applied to the integration of the equations. This results in the solution, at each step of the procedure, of a system of linear algebraic equations involving perhaps several hundred unknowns.

Finite difference schemes are often used for solving steady and unsteady gas dynamics equations. Lagrangian and Eulerian approaches are widely used here. In the first case, where the coordinate network is related to the fluid particles the structure of the flow is better defined and one succeeds in constructing rather accurate numerical schemes for flows with comparatively small relative displacements. In the second case, when the calculational network is fixed over space, the schemes are used for constructing flows with large deformation. In recent time, the approaches mentioned here have also found a wide application to the calculation of steady flows.

II. Method of Integral Relations. In this method, which is a generalization of the well-known method of straight lines, the region of integration is subdivided into strips by a series of curves, the shape of which is determined by the form of boundaries of the region. The system of partial differential equations written in divergence form is integrated across these strips, the functions occuring in the integrands being replaced by known interpolation functions. The resulting approximate system of ordinary differential equations is integrated numerically. The method of integral relations, like the method of finite differences, is applicable to equations of various types.

III. Method of Characteristics. This method is usually only applied to the solution of equations of hyperbolic type. The solution, in this case, is computed with the aid of a grid of characteristic lines, which is constructed in the course of the computation. Actually, the method of characteristics is a difference method of integrating systems of hyperbolic equations on the characteristic calculational network and is mainly used for detailed description of flows. Its distinguishing feature as compared to other difference mentods is the minimal utilization of interpolation operators and associated with it the region of influence of the difference scheme closely approximating the region of influence of the system of differential equations. The smoothing of the profiles, inherent in difference schemes with fixed network, is minimized since the calculational network used in the method of characterisitics is constructed exactly with the region of influence of the system taken into account.

Irregularity (nonconservativeness) of the calculational network should be noted as a drawback of the method of characteristics. It is

possible to develop a technique, based on this method, in which the calculations are carried out in layers bounded by fixed lines. The method of characteristics permits one to accurately determine the point of origin of secondary shock waves within the field of flow as the result of intersection of characteristics of one family. On the other hand, if a large number of such shock waves occur, difficulties are encountered in their calculation. Accordingly, the method of characteristics is most expediently applied to hyperbolic problems in which the number of discontinuities is small (for example, problems concerning steady supersonic gas flow).

IV. "Particle-in-Cell" Method (PIC). In certain respects, the PIC method incorporates the advantages of both the Lagrangian and Eulerian approaches. The range of solution here is separated by the fixed (Eulerian) calculation network; however, the continuous medium is represented by a discrete model, i.e., the population of particles of fixed mass (Lagrangian network of particles) which move across the Eulerian network of cells is considered. The particles are used to determine parameters of the fluid itself (mass, energy, velocity), whereas the Eulerian network is employed for determining parameters of the field (pressure, density, temperature).

The PIC method allows us to investigate complex phenomena of multicomponent media in dynamics, because particles carefully monitor free surfaces, lines of separation of the media, etc. Due to discrete representation of a continuous medium (the finite number of particles in a cell) calculational instability (fluctuations) often occurs. However the calculation of rarefied regions is also difficult. Limitations in capacity of modern computers do not permit a significant increase in the number of

particles.

For problems in gas dynamics involving a uniform medium, it seems more reasonable to employ the concept of continuity considering the mass flow across the boundaries of Eulerian cells instead of "particles".

Only numerical methods using high speed computers and careful experiments allow us to obtain the complete solution to complex gas dynamics problems and to determine the necessary flow characteristics. Thus, the elaboration of numerical schemes, the calculation of different gas dynamics problems, as well as the study of analytical properties of the solutions and their asymptotic behavior are of significant interest at present.

1.2 Aerodynamic Characteristics of High-Speed Vehicles.

In this paper a short review of the numerical methods used for the determination of the aerodynamic characteristics of high-speed vehicles with transonic and supersonic velocities will first be given. The numerical schemes were developed under our supersivion and in collaboration with the Moscow Physical Technical Institute and the Computing Center of the Academy of Sciences of the USSR. We shall discuss the problems of the development and use of the numerical algorithms for carrying out serial calculations in solving modern engineering problems arising in practice.

I. Steady-State Schemes. In determining the steady aerodynamic characteristics of bodies (especially when electronic computers of average capacity were employed) we made wide use of the following methods for solving the steady gas dynamics equations: the method of integral relations (m.i.r.), the method of characteristics (m.ch.) and some finite difference schemes (e.g., schemes with "artificial viscosity"). We wish to especially consider problems in which different discontinuities and singularities are

given beforehand, together with some associated boundary conditions; the solutions being carried out in regions where functions vary continuously.

Three different schemes of the method of integral relations have been developed for the determination of flow in the nose region of a blunt body, namely, one that employs an interpolation of various functions across the shock layer (Scheme I), along it (Scheme II) or in both directions (Scheme III). As a result the boundary value problem is solved for an approximate system of ordinary differential equations (Schemes I and II) or algebraic equations (Scheme III). To solve the three dimensional problem, certain additional trigonometric approximations in the circumferential coordinate were introduced. The various schemes of the method of integral relations have found a wide variety of applications [1-6].

The main advantage of these schemes is that, by means of different transformations, one succeeds eventually in approximating functions (or groups of functions) with comparatively weak variations. Consequently reliable results with a high degree of accuracy can be obtained with a comparatively small number of interpolation nodes (usually 3-4 are used).

The choice of the independent variables, the form of the initial system of equations of motion (i.e., the introduction of the integrals into the initial system and the use of the divergence form of the laws of conservation), the use of conservation schemes, the approximation of the integrals, etc., are all of great importance in writing an efficient numerical algorithm using m.i.r. .

The main difficulty in carrying out the schemes of m.i.r. is the solution of many parameter boundary value problems for the approximating system of equations. This is overcome by means of appropriate iteration

schemes. Moreover, these schemes have been used in transonic regions mainly for bodies of a comparatively simple form, while when dealing with a supersonic zone one has to adopt another algorithm.

In calculating supersonic flow the two- and three-dimensional schemes of the method of characteristics by P.I. Chushkin, K.M. Magomedov, and their co-workers were used [7,8]. With the governing equations expressed in characteristic variables, one requires approximation of ordinary derivatives, only. Using a fixed computational network, a system of linear finite difference equations is obtained with its attendant advantages.

With the help of the methods cited above, a large number of gas dynamics problems have been solved, namely, ideal gas flows with chemical reactions and radiation, transonic and three-dimensional flows, as well as viscous flows. In most cases reliable results were obtained which were in excellent agreement with experiment [6]. However, these approaches to the solution of the steady-state equation may be successfully used only for problems in which there are no singularities, discontinuities, intersections, and interactions. The application of these approaches is difficult for bodies of complex form with a large number of discontinuities. Besides, a single algorithm for the calculation of different types of flow is preferable.

II. Unsteady-State Schemes. The next step in the evolution of numerical methods, which was motivated by urgent practical needs and aided by the availability of electronic computers, was the development of nonsteady schemes to calculate the asymptotic solution of steady-state aerodynamic problems. In approximating the nonsteady equations, the general principles and ideas of the m.i.r. and m.ch. were applied with respect to space

variables. The divergence or characteristic forms of the initial equations were used and the same calculational networks were employed.

In this way the nonsteady Schemes II and III of the method of integral relations and the network-characteristic method were developed [9,10]. In this way rather complicated types of flow could be treated with a single algorithm. It is natural that the problems of computational stability and the attainment of steady-state solutions should become crucial. They require some specific technique such as the introduction of artificial viscosity into the initial system, and of dissipation terms into the difference equations. In a number of cases the accuracy of the results obtained is somewhat less than in the steady-state methods, but these approaches enabled us to consider new classes of problems; for example, the determination of the aerodynamic characteristics of specific configurations involving three-dimensional flow, the calculations of viscous transonic flows, and others [10].

III. "Large Particles" Method. Finally, in the third stage of development it seemed reasonable and advantageous to introduce the elements of the Harlow "particle-in-cell" method [11-13] into the algorithms. At first only the equation of continuity is represented as the mass flow across the Euler cell, using the simplest finite difference or integral approximation along the coordinates.

Thus the modified method of "large particles" [14-15] came into existence, which (again by means of the stability process) allowed us to consider from one point of view such a complicated task as, for example, the supsonic, transonic, and supersonic flow past a flat-nosed body in two dimensions or with axial symmetry. This method is likewise used in calculating viscous flows which would even permit the study of separated flows

from solutions of the Navier-Stokes equations [16-18].

The main principle of splitting the evolution of a physical process by a time step is as follows.

The medium simulated may be replaced by a system of N particles (fluid particles for a continuous medium and molecules for a discrete one) which at the initial instant of time are distributed in cells of the Eulerian mesh in a coordinate space in accordance with the initial data. The evolution of such a system in time Δt may be split into two stages: change of the internal state of sub-systems in cells which are assumed to be "frozen" or stable ("Eulerian" stage for a continuous medium and collision relaxation for a discrete one) and subsequent displacement of all the particles proportional to their velocity and Δt without changing the internal state ("Lagrangian" stage for a continuous medium and free motion of molecules for a discrete one). The stationary distribution of all the medium parameters is calculated after the process attains steady state.

It should be stressed that the development of the numerical schemes mentioned above has been paced by the improvement and extension of the ways of solving the boundary value problems for the corresponding approximating equations; by the consideration of a new, wider class of problems; by the development and improvement of electronic computers, machine languages, input and output arrangements, etc.

1.3 Computational Experiments

In recent years the introduction of big computers has aroused a considerably greater interest in various numerical methods and algorithms whose realization borders on carrying out computational experiments. The need in such an approach for the solution of problems of mathematical

physics is prompted by ever growing practical demands; in addition it is connected with an attempt of constructing more rational general theoretical models for the investigation of complex physical phenomena.

Let us outline the principle steps of computational experiments. At first, one chooses a mathematical model of a physical object based on its analytical study. Then one works out a tool for the investigation of the phenomenon in question, namely a difference scheme which permits the experiment itself to be carried out, i.e., the computational process. The next step comprises a detailed analysis of the results, leading to improvements and corrections of the mathematical model. This feedback procedure leads to perfections and modifications in the methodology of numerical experiments.

A close analogy to physical experiments comprising similar steps is evident; an analysis of the phenomenon under study; development of an experimental scheme; modification of design elements of the experimental installation; and measurements and their analysis.

In recent years the Computing Center of the USSR Academy of Sciences carried out a number of experiments associated with studies of complex gasdynamic flows using the non-stationary method of "large particles" [14,15]. Characteristic features of flows past bodies of different shapes were studied over a wide range of velocities, from subsonic, through transonic, up to hypersonic. In this paper results of a number of such experiments are presented without delving into the details of the computations [10,14,15,19,20].

It also seemed promising to apply the main principles of the approach in question for the simulation of rarefied gas flows. The application of

a statistical variant of such an approach for the solution of the Boltzmann equation is studied in [21-23]. Since the complete details of the techniques are given in the cited references, this paper will only be concerned with the characteristic features of each approach.

2. "Large Particles" Method for the Study of Complex Gas Flows.

For numerical models constructed by Yu.M. Davidov [14,15] on the basis of Eulerian equations, the mass of a whole fluid (Eulerian) cell, i.e., "a large particle" (from which originates the name of the method) is considered instead of the ensemble of particles in cells. Furthermore, non-stationary (and continuous) flows of these "large particles" across the Eulerian mesh are studied by means of finite-difference or integral representations of conservation laws.

This method utilizes the conservation laws given in the form of balance equations for a cell of finite dimensions (which is the usual procedure in deriving the gas dynamics equations but stops short of passing in the limit to a point. As a result, we obtain divergence-form conservative and dissipative-steady numerical schemes that allow us to study a wide class of complex gas dynamics problems (transonic flows, turbulent flows in the wake of a body, diffraction problems, etc.) [10,14,15,20].

2.1 Description of the Method

Consider the motion of an ideal compressible gas. Our starting-point is provided by the Euler differential equations in divergence form (the equations of continuity, momentum and energy)

$$\begin{aligned}
&\frac{\partial \rho}{\partial t} + \nabla \cdot (\rho \vec{V}) = 0, \\
&\frac{\partial \rho u}{\partial t} + \nabla \cdot (\rho u \vec{V}) + \frac{\partial p}{\partial x} = 0, \\
&\frac{\partial \rho v}{\partial t} + \nabla \cdot (\rho v \vec{V}) + \frac{\partial p}{\partial y} = 0, \\
&\frac{\partial \rho E}{\partial t} + \nabla \cdot (\rho E \vec{V}) + \nabla \cdot (p \vec{V}) = 0.
\end{aligned} \tag{1}$$

It was shown in [14] that, in the "large particle" method, the set of equations of gas dynamics, written as laws of conservation in integral form,

may be used instead of (1). The important point is that the difference scheme approximating the initial set of equations should be homogeneous, so that "through" computations may be performed without isolating singularities.

Equations (1) are completed by the equation of state

$$p = p(\rho, E, \vec{V}) = 0. \tag{2}$$

The various stages of the computational cycle will be considered separately. Let us briefly describe the main principles of the "large particle" method. The region of integration is covered by a fixed (over space) Euler mesh composed of rectangular cells with sides Δx, Δy (or Δz, Δr in a cylindrical coordinate system).

In the first ("Eulerian") stage of calculations only those quantities change which are related to a cell as a whole, and the fluid is supposed to be momentarily decelerated. Hence, the convective terms of the form $\mathrm{div}(\Phi\rho\vec{V})$ where $\Phi = (1, u, v, E)$, corresponding to displacement effects, are omitted in equation (1). Then it follows from the equation of continuity, in particular, that the density field will be "frozen" and the initial system of equations will be of the form

$$\rho \frac{\partial u}{\partial t} + \frac{\partial p}{\partial x} = 0, \quad \rho \frac{\partial v}{\partial t} + \frac{\partial p}{\partial y} = 0, \quad \rho \frac{\partial E}{\partial t} + \nabla \cdot (p\vec{V}) = 0. \tag{3}$$

Here we have used both the simplest finite-difference approximations and, to improve the calculation stability, the schemes of the method of integral relations, in which "sweeping-through" approximations of the integrands with respect to rays ($N = 3, 4, 5$) are used.

In the second ("Lagrangian") stage we find mass flows across the cell boundaries at $t^{n+1} = t^n + \Delta t$. At this stage we assume total mass to be transferred only by a velocity component normal to the boundary. Thus,

for instance

$$M^n_{i+\frac{1}{2},j} = \left\langle \rho^n_{i+\frac{1}{2},j} \right\rangle \left\langle u^n_{i+\frac{1}{2},j} \right\rangle \Delta y \, \Delta t \qquad (4)$$

The angle brackets $\langle \ \rangle$ denote the value of ρ and u on the cell boundary. The choice of these values is extremely important since they substantially influence the stability and accuracy of the computation. The various possible ways of writing down ΔM^n are characterized by consideration of the flow direction.

First and second order accurate representations of ΔM^n are considered. These are based on central differences, without account being taken of the flow direction, as well as by means of the discrete model of a continuous medium comprising a combination of particles of a fixed mass in a cell [14,15].

Lastly, in the third ("Final") stage we estimate the final fields of the Euler flow parameters at the instant of time t^{n+1} (all the errors in the solution of equations are "removed"). As was pointed out, the equations at this stage are laws of conservation of mass M, momentum $\vec{P}$ and total energy written down for a particular cell in the difference form

$$F^{n+1} = F^n + \Sigma \, \Delta \, F^n_{bdry}, \quad \text{where } F = (M, \vec{P}, E) \qquad (5)$$

According to these equations, inside the flow field there are no sources or sinks of M, $\vec{P}$ and E and their variation in time Δt is caused by interaction at the external boundary of the flow region.

2.2 Boundary Conditions.

To retain the unified nature of the computations and avoid special expressions for the boundary cells, layers of fictitious cells are introduced along all the boundaries, which are assigned parameters from the neighboring flow cells. The number of such layers depends on the order

of the difference scheme (one layer for the scheme of first-order accuracy, etc.). Two kinds of boundary then have to be distinguished: the rigid boundary (or axis of symmetry) and the "open" boundary of the computational region.

In the first case, the velocity component normal to the boundary changes sign, i.e., non-penetration condition along rigid walls, while the remaining flow parameters are taken unchanged. However another type of boundary condition is possible, namely, walls without slip (condition of sticking). In this case both velocity components change sign and the entire velocity vector vanishes on the wall.

Fluid can flow across "open" boundaries of the region, and some conditions on the continuity of the movement are required in this case. Consider the fluid to be flowing into the rectangular mesh from the left; then the parameters of the entering flow will be specified here. On the remaining "open" boundaries of the region we extrapolate the parameters of the flow "from within", i.e., transfer to the fictitious layer the parameter values from the layer nearest to the boundary (zero order extrapolation). A more complicated statement of the conditions is possible, or more accurate extrapolation (say linear or quadratic).

It is natural that the outer boundary of the region should be fairly remote from the source of disturbance, in which case methods of flow extrapolation "outwards" are possible. This topic will be discussed in more specific terms below. It will merely be mentioned here that the basic principle underlying the statement of the conditions is that no substantial disturbances should penetrate through the "open" boundaries of the region into the computational region.

2.3 Viscosity Effects.

It has already been remarked that this approach employs homogeneous

difference schemes, whereby computation by a unified algorithm is possible both through smooth flow regions and through discontinuities. This is achieved by using finite-difference schemes with a viscosity approximation. Let us dwell briefly on this topic.

While the equations of gas dynamics for a non-viscous gas were taken as the governing equations, viscosity effects are in fact inherent in our difference scheme. They are produced, firstly, by the introduction into the scheme of an explicit term with artificial viscosity ("viscosity pressure") and secondly, by the presence of an essentially schematic viscosity, dependent on the structure of the finite-difference equations.

The form of the approximation viscosity and estimates for the stability of the scheme can be obtained by writing as Taylor series the difference operators appearing in the equations in all three stages. The terms of zero (lowest) order should then represent the initial differential equations, while the structure of the approximation viscosity can be determined by retaining higher order terms in the expansions ("expansion errors"). The resulting differential equations will be termed the differential approximation of the finite-difference scheme, while an expansion up to second order terms in time and space is termed the first differential approximation [14,15,24].

The stability of the difference schemes may be investigated by means of the differential approximation. Such investigations were made by N.N. Yanenko and Y.I. Shokin for one-dimensional quasi-linear equations of the hyperbolic type [24]. While a strict mathematical foundation has not yet been supplied for the case of non-linear equations, the method of differential approximations has in fact been used here [13].

Taking the one-dimensional case for simplicity, let us describe the first differential approximation of our difference scheme. Take, say u^n_{i+1}, write it as function $u(x + \Delta x,t)$, and expand each term of the finite-difference equations in Taylor series in the neighborhood of the point (x,t).

For instance, in computations of ΔM^n from the expressions (4) of second order accuracy we obtain

$$\begin{aligned}
&\frac{\partial \rho}{\partial t} + \frac{\partial \rho u}{\partial x} = 0,\\
&\frac{\partial \rho u}{\partial t} + \frac{\partial (p + \rho u^2)}{\partial x} = -\frac{\partial q}{\partial x} + \frac{\partial}{\partial x}\left(\rho\varepsilon \frac{\partial u}{\partial x}\right), \qquad (6)\\
&\frac{\partial \rho E}{\partial t} + \frac{\partial}{\partial x}[u(p + \rho E)] = -\frac{\partial qu}{\partial x} + \frac{\partial}{\partial x}\left(\rho\varepsilon \frac{\partial E}{\partial x}\right),
\end{aligned}$$

or when using expressions (4) of first order accuracy

$$\begin{aligned}
&\frac{\partial \rho}{\partial t} + \frac{\partial \rho u}{\partial x} = \frac{\partial}{\partial x}\left(\varepsilon \frac{\partial \rho}{\partial x}\right),\\
&\frac{\partial \rho u}{\partial t} + \frac{\partial (p + \rho u^2)}{\partial x} = -\frac{\partial q}{\partial x} + \frac{\partial}{\partial x}\left(\varepsilon \frac{\partial \rho u}{\partial x}\right) + \rho\varepsilon \frac{\partial^2 u}{\partial x^2}, \qquad (7)\\
&\frac{\partial \rho E}{\partial t} + \frac{\partial}{\partial x}[u(p + \rho E) = -\frac{\partial qu}{\partial x} + \varepsilon \frac{\partial^2 (\rho E)}{\partial x^2} + \left(\frac{\partial \varepsilon}{\partial x}\right)\left(\frac{\partial \rho E}{\partial x}\right),
\end{aligned}$$

where $\varepsilon = |u|\Delta x/2$. The differential approximations may be written down similarly in the case of two-dimensional problems.

On the left-hand sides of (6) and (7), the exact expressions of the initial differential equations have been obtained, while on the right we have the terms which are a consequence of "viscosity" effects in the difference equations. The terms involving q result from the explicit introduction of an artificial viscosity, while the terms involving ε are due to schematic viscosity, which appears when the exact differential equations

are replaced by finite-difference equations ("expansion errors").

It may easily be seen that, as the mesh is refined ($\Delta x \to 0$), $\varepsilon \to 0$ and the equations of the differential approximation reduce to the exact set of initial equations. In practical computations (due to Δx, Δt,..., being finite), terms containing ε always appear implicitly in the difference scheme even when $q = 0$, which are in turn analogous to the dissipative terms of the Navier-Stokes equations. The role of the coefficient of actual viscosity is here played by the coefficient ε of schematic viscosity, which depends on the local flow velocity and the size of the difference mesh.

In the two-dimensional case, it follows from the equations of momentum that the schematic viscosity (with q = o) has the tensor form

$$\Delta = \frac{\rho}{2} \begin{Vmatrix} u\Delta x \frac{\partial u}{\partial x} & v\Delta y \frac{\partial u}{\partial y} \\ u\Delta x \frac{\partial v}{\partial x} & v\Delta y \frac{\partial v}{\partial y} \end{Vmatrix} = \frac{1}{2}\rho \vec{V}\, \Delta\vec{r} \cdot \nabla\vec{V}, \qquad (6')$$

where $\Delta\vec{r} = \Delta x\hat{i} + \Delta y\hat{j}$

It is clear from (6') that, due to the presence of the vectors $\Delta\vec{r}$ and $\vec{V}$, the schematic viscosity does not possess invariance under Galileo transformations; in practice it only appears in zones where the gradient is large, i.e., in a shock wave, at the body surface, and near flow separation. The coefficient of schematic viscosity ε (and hence the width of the "smeared" shock wave) then depends on the size of the local flow velocity and the cell size. In regions of smooth flow, where the gradients of the flow parameters are relatively small, the influence of the schematic viscosity is negligible.

It will be shown that in certain cases (when expressions (4) of

the first order accuracy are used for computing ΔM^n, the schematic viscosity ensures a stable computation even in the absence of pseudo-viscosity q; whereas when the second-order expressions (4) are used in regions where the local velocity is small compared with the velocity of sound, the introduction of a term with q is necessary to obtain a stable solution.

2.4 Stability of the Scheme.

While it is natural for different types of difference equations to be appropriate at various stages, the computations become strongly unstable on occasions, and rapidly increasing and oscillating solutions appear, which no longer reflect the behavior of the solutions of the initial differential equations.

The difference schemes quoted above are of the multi-layer type, while the difference equations are strongly non-linear with variable coefficients. This makes it impossible to employ Fourier's method, devised for linear equations with constant coefficients, for investigating the stability of the difference scheme as a whole. In essence, Fourier's method presupposes that the equations are linearized in the neighborhood of the flow with constant parameters, and it ignores non-linear effects (influence of the flow gradients), which are sometimes the true sources of the instability.

A heuristic approach will therefore be employed here to analyze the stability of the difference schemes, based on a consideration of their differential approximations [13,14,15] and appropriate for non-linear equations. In this approach, we determine the signs of the coefficients α_i ("diffusion coefficients") in the dissipative terms of the differential approximation; these terms contain second partial derivatives in the space

variables. For example, a linear equation can be indicated, such that, when the value of the coefficient is negative, the equation of the differential approximation admits a solution which is exponentially increasing in time (unstable) [14].

In short, the necessary conditions for stability are obtained here from the condition $\alpha > 0$ (parabolicity condition). In the case of linear equations, the results of a stability analysis obtained by means of the differential approximation are exactly the same as that obtained by Fourier's method.

Let us examine how the different ways of writing the continuity equation (second stage of the computations) contribute to the instability, assuming that the equations of momentum and energy are stable.

If ΔM^n is determined from the second order accurate expressions of (4), we find, on expanding the relevant difference equations in Taylor series and retaining terms containing $\partial^2\rho/\partial x^2$:

$$\frac{\partial \rho}{\partial t} + \frac{\partial \rho u}{\partial x} = \Delta_1 - \frac{\Delta t}{2}\,(u^2 + c^2)\,\frac{\partial^2 \rho}{\partial x^2} \quad . \tag{8}$$

If ΔM^n is evaluated from the first order accurate expressions of (4), we get

$$\frac{\partial \rho}{\partial t} + \frac{\partial \rho u}{\partial x} = \Delta_1^* + \left[\frac{\Delta x}{2}\,|u| - \frac{\Delta t}{2}\,(u^2 + c^2) - \frac{\Delta x^2}{4}\,\frac{\partial u}{\partial x}\right]\frac{\partial^2 \rho}{\partial x^2} \quad , \tag{9}$$

where Δ_1 and Δ_1^* are terms of the first differential approximation proportional to Δx and containing the first derivatives. In our case [14,15],

$$\Delta x \simeq 0.071;\ \Delta t \simeq 0.0071;\ \rho_\infty = 1;\ u_{-\infty} = 1 \tag{10}$$

In practical computations, when shock waves, contact discontinuities and rarefaction wave appear,

$$\rho|u| \simeq 1; \qquad \left|\frac{\partial u}{\partial x}\right| \Delta x < 0.3; \qquad \left|\frac{\partial \rho}{\partial x}\right| \Delta x < 2.$$

It follows from this that the coefficient of $\partial^2\rho/\partial x^2$ in (9) is positive, whereas it is negative in (8), i.e., scheme (8) is computationally unstable, while scheme (9) is stable.

2.5 Some Practical Aspects of the Method

It follows from the very character of the construction of the calculation scheme that a complete system of nonstationary gas dynamics equations is essentially solved here, while each calculation cycle represents a completed process in calculating a given time interval. Besides, all the initial nonstationary equations as well as the boundary conditions of the problem are satisfied and the real fluid flow at the time in question is determined.

Thus, the "large particles" method allows us to obtain the properties of nonstationary gas flows and as a consequence of their stability characteristics their asymptotic state as well. Such an approach is especially applicable to problems in which a complete or partial development of physical phenomena with respect to time takes place. For example, in studying transonic gas flows and flows around finite bodies, flow in local supersonic zones, and separation regions develop comparatively slowly while the major part of the field develops rather rapidly.

In contrast to the FLIC - method [25] our investigation is wholly devoted to systematic calculations of a wide class of compressible flows involving transonic regimes; discontinuity, separation and "injected" flows, etc.

The divergence forms of the differential and difference equations are considered in the "large particle" method; different kinds of approximations are used in the 1st and 2nd stages; additional density calculations are introduced in the final stage, which helps to remove fluctuations and makes

it possible to obtain satisfactory results with a relatively small network (usually one to 2.5 thousand cells are used). All this results in completely conservative schemes, i.e., laws of conservation for the whole mesh region are an algebraic consequence of the difference equations. Fractional cells are introduced for the calculation of bodies with a curvature in the slope of the contour.

The investigation of these schemes (approximation problems, viscosity, stability, etc.) was carried out for the zero, the first and the second differential approximations [13-15]. These investigations show that the "large particle" method yields divergence-conservative and dissipative--steady schemes for "sweeping-through" calculations.

These enable us to carry out stable calculations for a wide class of gas dynamics problems without introducing explicit terms with artificial viscosity. It may be of particular significance in studying flows around bodies with a curvature in the slope of the contour since the ways of introducing explicit terms with artificial viscosity are different for whole and fractional cells. Moreover, by varying only the second stage of the calculation procedure we can arrive at the conservative "particle-in-cell" method so that the calculational algorithm is of general use.

As for discontinuities the approximate viscosity in the schemes (dissipative terms in difference equations) results in stable calculations with a "smearing" of shock waves over several computational cells and the formation of a wide boundary layer near the body. It should be stressed that the magnitude of the approximate viscosity is proportional to a local flow velocity and to the dimension of the difference mesh, therefore its effect is practically evident only in zones with large gradients.

2.6 Results of Numerical Computations

Some computational results obtained by the "large particle" method [20] for transonic and "supercritical" flows around profiles, plane and axisymmetrical bodies will now be described.

For purposes of this discussion the supercritical regimes of transonic flows around bodies will be characterized by the value of the critical Mach number of the oncoming flow M_∞^* (i.e., when a sonic point first develops on the body) as well as by the extent of the local supersonic zone (as compared to a characteristic dimension of the body) and by its intensity (say the maximum supersonic velocity realized in the zone).

Figure 1 (series 1.a - 1.h) presents the flow field patterns (lines M = const.) for a 24% circular arc profile ($\nu = 0$) extending from purely subsonic ($M_\infty = 0.6$) to supersonic regimes ($M_\infty = 1.5$). Successive flow fields for increasing M_∞ depict transition through the critical Mach number (here $M_\infty^* = 0.65$), and the formation and development of a local supersonic zone. The supercritical flow around this profile is observed in Fig. 1 (b)-(g) ($0.65 < M_\infty < 1$). One can distinctly see the position of the shock in the region of crowded lines M = const. which bound the local supersonic flow together with the sonic line (M = 1). The region of subsonic velocities is located behind the shock wave. When the velocity of the oncoming flow increases, the flow disturbances produced by the body die out at a large distance from the body. With $M_\infty > 0.9$ the zone becomes considerable both in size and in intensity (supersonic velocities up to M = 1.7 to 1.8 are attained) and in case of sonic flow (Fig. 1.g) the sonic lines (M = 1) extend to infinity.

The asymmetry of the whole flow pattern is noticeable (even at purely

subsonic velocities - Fig. 1.a) which results from non-potentiality of the flow (super-critical regimes) and from the presence of viscous effects as well (formation of a wake behind the body).

In the case of a supersonic flow around a profile (Fig. 1.h, $M_\infty = 1.5$) a shock wave ahead of the body develops which bounds the disturbed region. Behind the wave, subsonic velocites occur in the vicinity of the axis of symmetry, away from which the flow velocity along the contour of the body increases and, as a result, a "terminal" shock occurs near the stern of the body.

For comparison the results of calculations by the above method of a flow around a 24% axisymmetric "spindle-like" body ($\nu = 1$) are given in Fig. 2 (2.a-2.h) for $0.8 \leq M_\infty \leq 2.5$. In this case a critical regime already occurs at $M_\infty^* \approx 0.86$; local supersonic zones as compared to the plane case are less developed and of weaker intensity (for example, values of $M \sim 1.3$ to 1.4 are realized), although, naturally, the main features of a transonic flow are quite evident.

In Fig. 3 a comparison is given between the flow fields calculated by the above method (solid line) and those of the Wood and Gooderum experiment (dashed line) [26] for subcritical (Fig. 3.a, $M_\infty = 0.725$) and supercritical (Fig. 3.b $M_\infty = 0.761$) flows around a 12% profile (results of both the calculations and the experiment indicate $M_\infty^* = 0.74$).

The analysis of internal check tests as well as the results of comparisons indicate that the computational error of the "large particle" method usually does not exceed several per cent. The calculations were carried out using a Soviet BESM-6 computer; the time of the calculation in this case did not exceed an hour.

Figures 4 to 6 show results of calculations for some complicated flows past bodies of different shapes in the presence of discontinuities in the wake as well as under the influence of injection of a fluid upstream from the front surface of the body. Such flows are of great practical interest in the study of wakes and turbulence.

The results of numerical experiments for the investigation of flows with injection, are given in Figs. 4a, 5 and 6b,c. They include the case of the interaction of a supersonic flow around a finite thick circular disk (Fig. 4a, $M_\infty = 3.5$), a 24% body of revolution (Fig. 5, $M_\infty = 3.5$), and a sphere (Fig. 6b, $M_\infty = 3.5$; Fig. 6c, $M_\infty = 6$) with a sonic injection stream (i.e., one where $M_c = 1.0$; $\rho_c = 2.9$, $u_c = 1.0$, $v_c = 0$) issuing upstream out of a nozzle situated on the axis of symmetry of the body. Fig. 6d presents results for the case when distributed injection of the flow takes place at the surface of a sphere. In all the figures, streamlines, shock waves, horizontal velocity lines (dots), and sonic lines (circles) are indicated; dashes denote lines separating the main flow from the injected stream.

The action of the jet markedly complicates the flow pattern. For instance, in the flow past a cylinder the head shock wave ABCD (Fig. 4a) is pushed towards the oncoming flow, and its distance from the body increases significantly. The jet issues out of the body in the direction of axis of symmetry at a sonic velocity and expands, forming a local supersonic region OLMNPO which is closed by a triple-shock intersection (normal front: ML; oblique front:MN; transverse front:MP), having a common point M. A recirculation zone with a complicated vortex structure developes in front of the body; sonic line BQ is situated much lower in comparison to flow

without injection. Behind the front recirculation zone, a secondary shock QC is formed and at some distance from the body merges with the head shock wave ABCD at point C.

Behind the bodies in Figs. 4-6, both with and without injection, one can observe the development of separated zones of recirculating flows. In the cases considered, these zones are closed, localized in the wake of the body and separated from the external flow by a "non-flow" line, i.e., a contact surface indicated by dashes in the figures. In the vicinity of the separation (it is interesting to note that in Fig. 4 the separation point is situated somewhat lower than the rear shoulder of the body) a transverse shock wave FF develops. Backward recirculation flows are essentially subsonic and rarefied (gas density and pressure are low), so that effects of viscosity are negligible.

The "large particle" method has also been applied to the study of internal gas flows and diffraction problems. Fig. 7 presents results of computations for flow through a straight channel ($\nu = 0$, Fig. 7a) and a straight tube ($\nu = 1$, Fig. 7b) in the presence of a central body ($M_\infty = 1.5$) for the case when a triple shock intersection is formed as a result of the interaction of the flow with the upper wall (this can be seen by an examination of the lines M = constant in Fig. 7a and rot $\vec{W}$ = constant in Fig. 7b).

In calculating separated flows, the cell dimensions of the "large particles" were changed several times so that across the wake of a body of size R from 4 to 30 computational intervals were used (Fig. 8). In all cases there was an ample reserve of computational stability (over 100 x Courant, where the Courant number represents the ratio of the time step to

the space width of the cell).

Fig. 8 shows base flows behind an axisymmetric cylinder ($M_\infty = 2.0$) for $R = 14\Delta y$. A gradual development of the flow in time is shown (in dimensionless units) from $t^n = 21$ to $t^n = 31$, when the zone is practically located. Streamlines are represented by solid lines; velocity vectors by arrows. It follows from this diagram that at $t^n \approx 25$ the flow has already been formed but still continues to "breathe". It is interesting to note that similar flow patterns were obtained with denser meshes (which is quite important) and the zone "breathing" i.e., changes of its dimensions, internal structure, and other features of the flow occurred approximately at the same time intervals, t^n, in the various approximations.

The development of flow separation in the case of strong interaction seems to be explained by the fact that, as a result of viscosity (computational) effects and the treatment of the boundary conditions, close to no-slip conditions are realized on the body itself; a fairly thick boundary layer forms around the body surface (comparable to the width of the body at its tail), and this layer then separates from the body surface and forms a near wake flow with complicated vertical structure behind the base of the body. It must be empahsized that, while the boundary layer is in fact the result of viscosity effects in the scheme, in the wake itself the influence of the approximation viscosity ε (which is proportional to the local velocity and the size of the computational mesh, see above) is quite small, since in these zones only small values of the subsonic velocities are realized, while computations with different size meshes revealed only a slight change (within the limits of one step) in the zone contour.

The fact that the solution does not strongly depend on viscosity

$\varepsilon \simeq \rho/u/h$) shows, by the way, that flows corresponding to high Reynolds numbers can be treated by our methods of analysis. Thus, our calculations of separated zones might give quantitative information for "limiting" flows ($Re \to \infty$) as, for example, the calculation of shock waves by a scheme including viscous effects. Naturally, the accuracy of determining the characteristic features of such zones can be further increased, if necessary, by using the results of preliminary calculations (e.g., the position of separation and closure points, a zone contour, etc.) as initial data.

However, it should be pointed out that in the calculations, the flow parameters on the front part of the body are determined comparatively quickly, while local supersonic zones and separation regions continue, as mentioned above, to "breathe". This may be due to the physical (non-stationary) character of the phenomenon itself. The application of the difference scheme of calculations prescribed by the non-stationary method of "large particles" appears to be especially well suited for such a case.

3. Computation of Incompressible Viscous Flows.

At the present time, a fairly large number of numerical methods of solving the Navier-Stokes equations (governing viscous incompressible flows) are known. Most of these methods were developed for equations expressed in terms of the stream function Ψ and vorticity ω.

A common disadvantage of these methods is the need for some form of a boundary condition (the Tom condition) for the vorticity on the solid surface, which is absent in the physical formulation of the problem. The rate of convergence of numerical algorithms is limited by the presence of an additional iteration imposed by this boundary condition on the surface vorticity.

Moreover, the obvious limitation of methods of solving the (Ψ,ω)-system, connected with their inapplicability for cases of three-dimensional viscous flows and compressible gas flows, accounts for the recent interest in the numerical solution of Navier-Stokes equations expressed in natural variables:

$$\frac{\partial \vec{V}}{\partial t} + (\vec{V}\cdot\nabla)\vec{V} = -\Delta p + \nu\Delta\vec{V}, \quad \nabla\cdot\vec{V} = 0 \tag{11}$$

where p - pressure, $\vec{V}$ - vector of velocity, ν - coefficient of kinematic viscosity.

Using the main principles of the "large particle" method V.A. Gushchin and V.V. Shchennikov [16,17,29] studied viscous incompressible gas flows with variables "velocity-pressure" by means of a numerical scheme of splitting analogous to the SMAC method [27].

3.1 Description of the Splitting Method

Let us now consider the scheme of difference approximations of equations (11) which enable calculations by a single algorithm for plane, axisymmetric and three-dimensional flows of a viscous incompressible fluid.

For this purpose consider the following scheme of splitting a time cycle:

Stage I - determination of intermediate values of velocities

$$(\tilde{\vec{V}} - \vec{V}^n)/\tau = -(\vec{V}^n \cdot \nabla)\vec{V}^n + \nu\Delta\vec{V}^n \ ; \qquad (12.1)$$

Stage II - calculation of the pressure field

$$\Delta p = \Delta\tilde{\vec{V}}/\tau \ , \qquad (\nabla \cdot \vec{V}^{n+1} = D^{n+1} = 0) \ ; \qquad (12.2)$$

Stage III - determination of the final values of velocities

$$\vec{V}^{n+1} = \tilde{\vec{V}} - \tau \cdot \nabla p \ . \qquad (12.3)$$

Stages I and III lead to the realization of the Navier-Stokes equation and stages II and III are the conditions of solenoidality (second equation of (11)). Consequently at stage I the evolution of the velocity field is accomplished only by convection and diffusion so that the resulting $\tilde{\vec{V}}$-field does not satisfy the continuity equation (i.e., $\tilde{D} \neq 0$). Therefore it is necessary to change ("to correct") the field $\tilde{\vec{V}}$ at the expense of a pressure gradient p so that $D^{n+1} = 0$ (stage III) where p is found by solving the Poisson equation (stage II).

For a proportional calculational mesh a two-dimensional difference scheme of second order accuracy with respect to space is presented in [17]. The main difficulties of the numerical realization of the scheme involve the calculation of a pressure field and the formulation of boundary conditions.

It should be noted that in some works boundary conditions at a solid surface are replaced by the projection of an equation of motion onto the normal to the surface at the boundary points. This substitution reduces the efficiency of the numerical methods since these conditions are not available in the physical formulation of the problem.

In [28] there is proposed an original modification of boundary conditions

in the MAC method, which enables homogeneous boundary conditions to be provided for pressure. Moreover, in the SMAC method [27] and the modified MAC method [28], due to the difference schemes chosen, the realization of the condition of no-slip necessarily results in the determination of the vorticity value on a solid surface which satisfies the Tom condition to first order accuracy. In addition, the no-slip condition in the SMAC method does not provide a balance of forces on a solid surface. The error in this case is of the order of $0(\nu)$.

An essential point of the method proposed is the choice of boundary conditions. From the viewpoint of the solution of problems of a viscous incompressible flow around bodies of finite dimensions we can distinguish two basic types of boundary conditions: conditions on a solid surface and those on a line sufficiently remote from the body. Let us consider each of these conditions in further detail.

Boundary conditions on a solid surface:

$$\begin{aligned} v^n_{i,-\frac{1}{2}} &= 0 \qquad \text{(nonpenetration condition)}, \\ u^n_{i+\frac{1}{2},-\frac{1}{2}} &= 0 \qquad \text{(no-slip condition)}; \end{aligned} \tag{13}$$

from the latter it follows

$$\tilde{u}_{i+\frac{1}{2},0} = \frac{u^n_{i+\frac{1}{2},0}}{2} + \frac{u^n_{i+\frac{1}{2},1}}{6} + 0(h^3) \tag{14}$$

Condition (14) makes it possible to determine the boundary value for $\tilde{u}$ of second order accuracy with respect to internal field points. This avoids the alternative of introducing a layer of fictitious cells (inside a solid body), which in schemes of the MAC, SMAC and modified MAC types [28] gives rise to only first order accurate values of surface vorticity. Note that in the limits of the approach proposed it is unnecessary to calculate the

vorticity on the solid surface. The latter can be determined from a calculated velocity field using some of the difference representations of the vorticity

$$\omega = \partial u/\partial y - \partial v/\partial x$$

at boundary points.

Boundary conditions on a line remote from the body represent an undisturbed flow; for $\bar{U}_\infty \| OX$ this has the form

$$v^n_{i,N+\frac{1}{2}} = 0, \quad u^n_{i+\frac{1}{2},N} = U_\infty$$

In calculating the pressure field, homogeneous boundary conditions are attained following the approach of [28]. Corresponding to $v^{n+1}_{i,-\frac{1}{2}} = 0$ (for the case of a solid surface) and $v^{n+1}_{i,N+\frac{1}{2}} = 0$ (for the case of a line remote from a body) we have from the finite-difference approximation of (12.3)

$$\tilde{v}_{i,-\frac{1}{2}} = \frac{\tau}{h}(p_{i,0} - p_{i,-1}), \quad v_{i,N+\frac{1}{2}} = \frac{\tau}{h}(p_{i,N+1} - p_{i,N}). \qquad (15)$$

Taking account of (15) it is not difficult to write down now a difference equation for calculating the pressure at boundary cells [17].

The stationary solution of the system of equations (12) is obtained as a result of repetition of the above stages until the following criterion is fulfilled

$$\max_{i,j} |u^{n+1}_{i+\frac{1}{2},j} - u^n_{i+\frac{1}{2},j}| \leq \varepsilon^*.$$

The stability can be investigated stage-by-stage. A stability criterion for the first stage can be obtained from the first differential approximation (condition of α-parabolicity). With regard to equations (12a) the first differential approximation is [17]:

$$\frac{\partial u}{\partial t} + \frac{\partial u^2}{\partial x} + \frac{\partial uv}{\partial y} = (\nu - \frac{\tau}{2} u^2)\frac{\partial^2 u}{\partial x^2} + (\nu - \frac{\tau}{2} v^2 - \frac{h^2}{4}\frac{\partial v}{\partial y})\frac{\partial^2 u}{\partial y^2},$$

$$\frac{\partial v}{\partial t} + \frac{\partial uv}{\partial x} + \frac{\partial v^2}{\partial y} = (\nu - \frac{\tau}{2} u^2 - \frac{h^2}{4}\frac{\partial u}{\partial x})\frac{\partial^2 v}{\partial x^2} + (\nu - \frac{\tau}{2} v^2)\frac{\partial^2 v}{\partial y^2} \qquad (16)$$

The stability criterion of the difference scheme employed follows from (16)

$$\tau \leq 4\nu/(u^2 + v^2)$$

Eliminating p from (12.2) and (12.3), the unconditional stability of the second and third stages is easily demonstrated by Fourier's method.

Thus, the proposed difference scheme enables us to calculate a flow without prescribing vorticity and pressure at the body surface. This markedly increases the accuracy of the calculations. Results of the calculations attest to its effectiveness. This difference scheme (of second-order accuracy) provides a single algorithm for calculating viscous incompressible flows around plane, axysymmetrical and three-dimensional bodies of complex configuration as well as internal flows in a wide range of Reynolds numbers [17].

3.2 Results of Numerical Computations

Solutions of a whole series of problems of external hydrodynamics were obtained by the method described. Viscous incompressible flows over a wide range of Reynolds numbers ($1 \leq Re \leq 10^3$) were studied around different bodies of finite dimensions: a rectangular slab and a cylinder of finite length whose axis is parallel to the free stream $\bar{U}_\infty$ [29], a sphere and a cylinder with the axis perpendicular to $\bar{U}_\infty$, a rectangular parallelepiped (a three-dimensional flow) [7], as well as bodies of more complex form.

Fig. 9 shows the steady-state streamline patterns around a circular cylinder (two-dimensional flow) for Re = 1,10,30 and 50($Re = 2Rv_\infty/\nu$, where

R is the cylinder radius). The streamline patterns in flow around a cylinder for Re = 10^3 are shown in Fig. 10 at the instants t_1 = 162, t_2 = 166 and t_3 = 170, respectively. In the last case a non-steady flow pattern is observed (there is a definite growth of the stagnation zone and at some instant of time occurs a "collapse" and ejection of fluid from the stagnation zone). This result probably requires further study.

Figs. 11 and 12 present results for unsteady three-dimensional incompressible viscous flow around a cube (of dimension 2a) when the oncoming flow velocity $\overline{U}_\infty$ is parallel to an axis OX. Due to the presence of two planes of symmetry (OXY and OZX) the calculation is carried out only in the positive quadrant OXYZ (Fig. 11). The properties of the flow are illustrated by the velocity profiles u(parallel to the vector $\overline{U}_\infty$) at various cross-sections Q (x = const.). Fig. 11 shows the velocity profile u in the undistrubed flow ($x = -\infty$) and for a section x = 3a with Re = 1 ($Re = 2a\, V_\infty / \nu$). Fig. 12a illustrates for various Re the spatial change of the velocity profiles u at several sections downstream of the body (section Q_1 coincides with the rear face of the cube x = 2a; the distance between the sections is constant, $\Delta x = 0.5a$). Fig. 12b shows the evolution with time ($1.0 \leq t \leq 1.29$) of the velocity field for the section x = 4a. It follows from Fig. 12, in particular, that with Re = 40 and 100 a reverse-circulation zone ($u < 0$) develops, and after an elapse of time a certain flow stabilization is observed. The reader is referred to [16,17,29] for further details concerning results of this calculation.

4. Flow of a Viscous Compressible Gas (Conservative "Flow Method")

The calculation of viscous compressible gas flows was performed by L.I. Severinov and A.I. Babakov with the approximation of conservation laws represented in integral form for each cell of the calculation scheme ("flow" method) [18]. Conservation laws for mass, momentum and energy of a finite volume have the form:

$$\frac{\partial F}{\partial t} = -\iint_{s_\Omega} \vec{Q}_F \, \vec{ds}, \qquad F = \{M,X,Y,Z,E\} \quad , \tag{17}$$

where s_Ω - is the lateral surface of volume cell Ω; M - mass, X,Y,Z, - momentum components and E - energy terms in Ω, respectively, and $\vec{Q}_F$ is a flow density vector for each of the quantities. Eqs. (17) take account of the boundary conditions and are solved numerically for each cell of the computational domain.

If the values of $M^n = M(t^n)$, X^n,Y^n,Z^n,E^n are known at the instant $t^n = n\tau$, where τ is a time integration step, at time $t^{n+1} = (n+1)\,\tau$ these quantities can be calculated with error $0(\tau^2)$ as follows [18]:

$$F^{n+1} = F^n - \tau \iint_{s_\Omega} \vec{Q}_F^{\,n} \cdot \vec{ds} \; . \tag{18}$$

Supplementary conditions, the form of which depends on the problems posed, must make it possible to determine the flow-density vectors on the boundary of the domain in which the solution is sought. The three-dimensional coordinate system, the shape of the cell volumes Ω, the methods of determining the field variables and their first derivatives on the surfaces s_Ω must be chosen in such a way as to ensure stability and monotonicity of the difference method, as well as a fairly simple approximation of the integrals in the system (18).

In the solution of a specific problem the integrals in (18) are calculated on separate segments of the surface which are the boundaries between two adjacent volumes Ω. Depending on the directions of the flow density vectors the values of M,X,Y,Z and E vary (they increase in some cells and decrease in others) by quantities determined by the flows of mass, momentum and total energy through the corresponding segments of the boundary. Apart from round-off errors this calculation method cannot lead to the loss or generation of the quantities {M,X,Y,Z,E} due to computational errors. Therefore, the flow method is conservative with respect to mass, momentum components and total energy [18].

In the finite-difference approximation of Equation (18) Stokes' assumption of the equality of the mean values of the principal stresses (with a reversed sign) and pressure has been used. If the field variables are sufficiently smooth and the assumptions used in calculating the mass, momentum and energy flow density vectors are satisfied, the conservation laws (17) imply the complete Navier-Stokes equations for a compressible gas, if the volume Ω is arbitrary.

4.1 Computational Problems

We will now consider some problems involved with the numerical investigation of equation (17).

Knowing the values of M,X,Y,Z,E for each cell, we can calculate for a given small volume cell Ω fixed in space the average densities (in each cell) of the given quantities $\rho,\xi,\eta,\zeta,\varepsilon$:

$$\rho = M/\Omega,\ \xi = X/\Omega,\ \eta = Y/\Omega,\ \zeta = Z/\Omega,\ \varepsilon = E/\Omega\ .$$

From these functions it is easy to arrive at generally accepted field varibles, i.e., the components u,v,w of the velocity $\vec{V}$ and the specific

internal energy of the gas e:

$$u = \xi/\rho,\ v = \eta/\rho,\ w = \zeta/\rho,\ e = \varepsilon/\rho - (u^2 + v^2 + w^2)/2.$$

Applying certain procedures of interpolation and numerical differentiation, we determine the value of the field variables and the first derivatives of u,v,w,e on the boundaries s of the cells Ω [18].

In determining the values of all the function (except the distribution densities $\rho,\xi,\eta,\zeta,\varepsilon$) and their first derivatives, symmetric formulas were used, for example,

$$u_{m+\frac{1}{2},k} = (u_{m+1,k} + u_{m,k}) / 2,$$

$$\left(\frac{\partial u}{\partial x}\right)_{m+\frac{1}{2},k} = (u_{m+1,k} - u_{m,k}) / h_1,$$

$$\left(\frac{\partial u}{\partial y}\right)_{m+\frac{1}{2},k} = (u_{m,k+1} - u_{m,k-1} + u_{m+1,k+1} - u_{m+1,k-1}) / 4h_2 .$$

However asymmetric formulas were used to calculate the density values of the distributions $\rho,\xi,\eta,\zeta,\varepsilon$:

$$\rho_{m+\frac{1}{2},k} = \begin{cases} 1.5\rho_{m,k} - 0.5\rho_{m-1,k} & \text{if } u_{m+\frac{1}{2},n} > 0 \ ; \\ 1.5\rho_{m+1,k} - 0.5\rho_{m+2,k} & \text{if } u_{m+\frac{1}{2},n} < 0 \ . \end{cases}$$

These approximations ensure second-order accuracy.

In approximating flow density vectors $\vec{Q}_F$ an essential aspect of the method required that the distribution densities of additive characteristics such as densities F are calculated on the boundary s_Ω of volume Ω in a non-symmetrical way (extrapolation in the direction of gas flow); while the other parameters, e.g., pressure and transfer velocities u,v of additive characteristics are calculated according to symmetric formulas in the viscous stress tensor and in the thermal conduction law. We believe that this treatment accounts for the region of influence, which is an important factor in the investigation of complex physical flow patterns. The presence of a "convective" transfer gives unequal weighting to the space directions and it is desirable to take account of this fact in constructing the difference scheme.

The integral form of the conservation laws essentially requires the

approximation of derivatives of one order lower than that required for numerical solutions of the Navier-Stokes equations. By its formulation the "flow" method is conservative with respect to mass, momentum and total energy, both locally (for each cell of a difference mesh) and integrally, i.e., for the whole computational space [18]. As follows from (17), conservativeness results from the fact that this approach is based upon the difference approximation of conservation laws written down for each cell in terms of surface integrals of vectors of flow densities $\vec{Q}_F$, i.e., the conservation law which governs an arbitrary gas volume. Indeed, while solving a given problem, surface integrals in (17) are calculated on separate surface segments s_Ω which constitute boundaries between two adjacent volumes Ω. Depending upon the direction of flow vectors the values F = {M,X,Y,E} vary (they increase in some cells and decrease in others) and acquire new values determined by flows of mass, momentum and total energy across common boundaries of the cells.

It should be noted that the "flow" method is essentially another development of the "large particle" method. The difference formulas of the "flow" method can be deduced by using the splitting scheme (3) - (5) for the "transfer" of the components of quantities F.

4.2 Examples of Calculations

The "flow" method has been applied to the systematic study of the characteristics of viscous compressible gas flow around bodies of finite dimensions over a wide range of Reynolds numbers Re. Although the method formally "works" even with large values of Re, the results are reliable only when the boundary layer thickness is much greater than the size of the computational mesh. It should be emphasized that the division of the

vector of flow density $\vec{Q}_F$ into convective and viscous components facilitates application of the algorithm to the calculation of an ideal gas flow, as well.

The results given below represent the asymptotic steady state obtained by the method for the solution of a stationary boundary value problem. The investigation of a linear model reinforced by the results of the calculations themselves showed that the second-order accurate difference scheme exhibited conventionally stability and monotonicity [18]. The reliability of the numerical results is examined for a general case by subdividing the computational cell, by using various forms of boundary conditions, by comparing with the results of other calculations as well as with measurements taken from an experiment [18,30].

Some details of the flow past a sphere (separation zones of a reverse-circulation) at M_∞=20 and $550 \leq Re_\infty \leq 10^4$ are given in Figs. 13 and 14. Fig. 14 shows the behavior of lines p = const. in a separation zone behind the sphere with $Re_\infty = 10^4$ and 1500 ($Re_\infty = Rv_\infty/\nu$).

Fig. 15 illustrates the variation of density across the shock layer in the neighborhood of the forward stagnation point ($x = 3^o$) for $75 \leq Re_\infty \leq 10^4$ and compared with that of an ideal gas ($M_\infty = 20$, $k = 1.4$, $Re_\infty = \infty$). With increasing Re_∞ the density in the shock layer approaches its limiting value in a viscous thermally non-conducting gas; the tendency towards the formation of a shock wave is distinctly seen.

The pressure distribution along a blunt body (relative to the pressure at the stagnation point, x = 0) is shown in Fig. 16: "lines" designate the results obtained by the "flow" method ($M_\infty = 6.05$, $Re_\infty = 6.43 \cdot 10^6$), "crosses" - experimental data (G.M. Riabinkova) and "circles" - the results for an

ideal gas (O.M. Belotserkovskii [31]). Very good agreement is observed between the data. In this way transition from the "viscous" equations (17) to the limit of an ideal gas is obtained.

The results of calculations show that the "flow" method makes it possible to study viscous compressible gas flows around finite bodies over a wide range of flow regimes (including separation zones) up to large Reynolds numbers.

5. Statistical Model for the Investigation of Rarefied Gas Flows

A statistical variant of the method of large particles has been investigated by V.E. Yanitsky [21-23] for the solution of the Boltzmann equation. The main difficulty of this problem is the development of a model of behavior of the gas medium consisting of a finite number of particles. This study combines the splitting of the "large particle" method in terms of Bird's statistical treatment [32,33] with Kats' ideas [34] about the existence of asymptotically equivalent models to the Boltzmann equation.

As is typical of "particle-in-cell" methods, the medium is simulated by a system containing a finite number N of particles of fixed mass. At a given instant of time t_α each cell j contains $N(\alpha,j)$ particles endowed with certain velocities. The main calculation cycle comprises two stages:

- at the first stage particles only collide with their counterparts in a cell (collisional relaxation) and

- at the second stage they are only displaced and interact with the boundary of a reference volume and with the surface of a body(collisionless relaxation).

The main distinction between the model suggested in [21-23] and Bird's model lies in the fact that at the first stage of the calculation each group of N particles in a cell is regarded as Kats' statistical model for an ideal monoatomic gas consisting of a finite number of particles in a homogeneous coordinate space. Molecular collisions are calculated by the Monte-Carlo method from the main equation of Kats' model, which correctly determines the time between particle collisions in accordance with collision statistics for an ideal gas.

In contrast to previously reported versions of Bird's method [32,33]

the approach in question [21-23] is a rigorously Markovian process. The main equation of this formulation is linear (unlike the Boltzmann equation), which substantially simplifies numerical realization of the algorithm. The feature of molecular chaotic motion implies that Kats' model is asymptotically equivalent to the Boltzmann equation without the convective derivative. Integration of Kats' main equation results (with accuracy up to the realization of the assumption of molecular chaotic motion) in the Boltzmann equation.

In the realization of the second stage of the calculation for the displacement of the particles, the numerical algorithms [21-23] employ incomplete information about the position of particles in coordinate space. This reduces storage requirements in the processor memory, which significantly increases the speed of the computations. The method can just as well be realized in a two- or three-dimensional coordinate space.

Let us review here the principal aspects of the statistical "particle--in-cell method [21-23].

5.1 Description of the Statistical "Particle-in-Cell" Method.

We suppose that the problem of a rarefied gas flow around a body can be solved by means of a distribution function with a monoatomic gas. Then any macroparameter of a gas flow $\Psi(t,\vec{x})$ related to a molecular feature $\Psi(\vec{c})$ is a functional of the form

$$\Psi(t,\vec{x}) = \frac{1}{n(t,\vec{x})} \int \Psi(\vec{c}) \cdot f(t,\vec{x},\vec{c})\, d\vec{c} \quad ,$$

where $f(t,\vec{x},\vec{c})$ is a molecular distribution function in a 6-dimensional space $(\vec{x},\vec{c})$ of the coordinates and velocites of the particles.

If Ω denotes the region of a control volume and Γ - the boundary of Ω which emcompasses a body surface as well, then the problem is reduced to

that of obtaining the solution of Boltzmann's equation

$$\frac{\partial f}{\partial t} + \vec{c}\ \frac{\partial f}{\partial \vec{x}} = \int (f' \cdot f'_j - f f_1)\ g d\sigma \cdot d\vec{c}_1 \quad , \tag{19}$$

subject to the initial parameters

$$f(t + 0, \vec{x}, \vec{c}) = f_o(\vec{x}, \vec{c}), \quad \vec{x} \in \Omega, \quad -\infty < c_{x,y,z} < +\infty \tag{20}$$

and boundary conditions

$$f(t, \vec{x}_\Gamma, \vec{c}) = \int \kappa(\vec{c}, \vec{c}_1) f(t, \vec{x}_\Gamma, \vec{c}_1) d\vec{c}_1; \quad \vec{c}\vec{n}(\vec{x}_\Gamma) > 0, \quad \vec{c}_1 \vec{n}(\vec{x}_\Gamma) < 0 \ . \tag{20'}$$

Here $\vec{n}(\vec{x}_\Gamma)$ is the normal to the surface Γ at point $\vec{x}_\Gamma \in \Gamma$ directed toward the interior of volume Ω; the kernal shape κ is derived from the interaction law of the "gas-surface".

In deducing Boltzmann's equation the following assumptions are made.

1) mechanics of collisions are described in a classical way;

2) force fields of molecules are spherically symmetric;

3) only binary collisions are considered (two molecules take part in any collision);

4) molecules move randomly (the hypothesis of molecular chaos is valid, i.e., the distribution function of molecular pairs $f_2(t, \vec{x}, \vec{c}_1, \vec{c}_2) = f_1(t, \vec{x}, \vec{c}_1) \cdot f_1(t, \vec{x}, \vec{c}_2)$ which implies statistical independence of particles);

5) the collision time is negligibly small.

The difficulty in constructing the solution of the Boltzmann equation in nonlinear integro-differential form results both from the large number of independent variables (there are seven of them in the general case: time, geometrical coordinates and molecular velocity components) and from the complex structure of the integral of the collisions. Quadratic nonlinearity in the integrands, their strong dependence upon distribution functions (determined by the values of molecular velocities after a collision) as well as

the high level of multiplicity of integration (equal to five in a general case) and the complex formulation of the boundary condition (20) - these are the main features which complicate a direct solution of the Boltzmann equation (19) and the application of ordinary numerical algorithms.

For an approximate solution of the problems formulated in this fashion we shall construct a statistical model of an ideal monotomic gas consisting of N particles* with coordinates r_i, and velocities $c_i (i = 1,2,\ldots,N)$ so that the equation of evolution of the model approximates equation (19), the only additional assumption being that of molecular chaos:

$$f_2(t,\vec{x},\vec{c}_1,\vec{c}_2) = f_1(t,\vec{x},\vec{c}_1)\cdot f_1(t,\vec{x},\vec{c}_2) \quad , \tag{21}$$

where

$$f_s(t,\vec{x},\vec{c}_1,\ldots,\vec{c}_s) \equiv \frac{N}{(N-S)!} F_s(t,\vec{r}_1,\ldots,\vec{r}_s,\vec{c}_1,\ldots,\vec{c}_s)$$

and with $r_1 = r_2 = \ldots = r_s = x$, F_s being a s-partial function of distribution in a phase space of 6N dimensions.

If $\{\vec{R}(t),\vec{c}(t)\} = \{\vec{r}_1(t),\vec{c}_1(t);\ldots;\ \vec{r}_N(t),\vec{c}_N(t)\}$ designates the model state at time t, the problem solution is then reduced to a numerical realization of a finite number of trajectories $\{\vec{R}(t),\vec{c}(t)\}$ with initial parameters corresponding to (20); the modelling of particle interaction with the boundary Γ is accomplished in accordance with the given kernel κ of (20'). Having calculated a number of trajectories one can obtain any macroparameter using adequate estimates of the integrals by the Monte Carlo method.

---

* A real gas is modelled by an ensemble of about a thousand rigid sphere-like molecules that can be regarded as typical representatives of many trillions (10^{12}) of molecules, e.g., in the study of phenomena occuring in a real shock wave [22].

The synthesis of the basic ideas of splitting, the "particle" method and Kats' statistical model enable us to construct the desired model $\{\vec{R}(t),\vec{c}(t)\}$ for a space-inhomogeneous case when $\partial f/\partial x \neq 0$.

Let us suppose that at time interval $t_\alpha (\alpha = 0,1...)$ in a cell with center $x_j (j = 1,2,...,j)$ there are $N(\alpha,j)$ particles with velocities $\{\vec{c}_1,...,\vec{c}_{n(\alpha,j)}\}$. The center x_j of a cell in which a particular particle is situated is taken as a coordinate r_i of a particle i. The state of such a gas model $\{\vec{R},\vec{c}\}$ is uniquely defined by a sequence of J points of the form:

$$\{\vec{R}(t),\vec{c}(t)\} \sim \{N(\alpha,j);\ \vec{c}_s,...,\vec{c}_{N(\alpha,j)}\}\ ,\ j = 1,2,...,J\ ,$$

$$N = \sum_{j=1}^{J} N(\alpha,j)\quad .$$

The evolution of this system in time Δt is split into two stages.

The first stage models the change of internal state of subsystems enclosed in the cells, assuming that the particles are fixed; collisions of particles (with their counterparts in a cell) in subsystems $\{\vec{c}_1,...,\vec{c}_N\}$ are simulated independently in each cell, thus the particles acquire new velocities. The vector $\vec{c} = \{\vec{c}_1,...,\vec{c}_N\}$ is regarded as a state of Kats' model. Let $\phi(t,\vec{c})$ be the density of the probabilistic distribution of the state $\vec{c}(t)$; then the governing equation of this model ("Kats' Master Equation" [24]) has the form

$$\frac{\partial\phi(t,c)}{\partial t} = \frac{1}{V}\sum_{1<\ell<m\leq N} g_{\ell m}\int[\phi(t,\vec{c}_{\ell m}) - \phi(t,\vec{c})]d\sigma_{\ell m} \equiv K\phi(t,\vec{c})\ . \quad (22)$$

where K - Kats' operator of collisions; $g_{\ell m} = |\vec{c}_\ell - \vec{c}_m|$, $\vec{c}_\ell$ and $\vec{c}_m$ denote the velocities of the ℓ-th and m-th particles upon their collision; $d\sigma_{\ell m}$ - a differential section of elastic dissipation of a pair of particles $(\vec{c}_\ell,\vec{c}_m)$; a normalizing parameter V is determined by the choice of measurement units and it can be interpreted as a cell volume.

If we introduce the distribution functions

$$f_s(t,\vec{c}_1,\ldots,\vec{c}_s) = \frac{N!}{(N-s)!V^s}\int\phi(t,\vec{c})\prod_{i=s+1}^{N} d\vec{c}_i \quad ,$$

then by integrating (22) it is not difficult to obtain

$$\frac{\partial f_1(t,\vec{c}_1)}{\partial t} = \int[f_2(t,\vec{c}_1',\vec{c}_2') - f_2(t,\vec{c}_1,\vec{c}_2)]g_{12}\cdot d\sigma_{12}\cdot d\vec{c}_2$$

which coincides with the Boltzmann equation having a zero convective derivative when satisfying equality(21).

The algorithm for the realization of the first calculational stage of evolution of a space-inhomogeneous model corresponds to the Monte Carlo method of numerical solution of Kats' basic equation (22) which (unlike the Boltzmann equation) is linear.

The second stage models a collisionless transfer of particles from a particular cell to any neighboring one without changing the internal state of the subsystems; their interactions with the control volume boundary and body surface are considered as well. This stage corresponds to the Monte Carlo method of numerical solution of the Boltzmann free-molecular equation in the following form

$$\frac{\partial f}{\partial t} + \vec{c}\,Lf = 0. \qquad (23)$$

where L is a finite-difference operator approximating the derivative $\partial/\partial x$; its introduction is closely related to an incomplete description of the system state in coordinate space.

The simplest numerical algorithms of the method described [21-23] correspond to the solution of time explicit, conventionally-stable finite--difference schemes of first-order accuracy, respectively, for Kats' equations and the Boltzmann free-molecular equation. Herein the equation of evolution of a model gas $\{R(t_\alpha), \vec{c}(t_\alpha)\}$ within the accuracy of satisfying

molecular chaos has the form (a one-dimensional flow)

$$\frac{\Delta_\alpha f}{\Delta t} + c_x \cdot \frac{\Delta_\alpha f}{\Delta x} = J(ff_1) - \Delta t c_x \frac{\Delta_\alpha J(ff_1)}{\Delta x} \qquad (24)$$

where $\Delta_\alpha / \Delta t$ and $\Delta_\alpha / \Delta x$ are first-order finite-difference operators approximating derivatives $\partial/\partial t$ and $\partial/\partial x$, respectively; $J(ff_1)$ designates the right-hand side of the Boltzmann equation. The finite-difference scheme given is conventionally-stable and it approximates the Boltzmann equation within the accuracy of $0(\Delta t)$ and $0(\Delta x)$. As mentioned above, this calculation employs incomplete information concerning the space position of particles.

This calculational model can naturally be extended to the cases of a two- and three-dimensional space; it consists of a sequence of one-dimensional displacements along each coordinate axes. This corresponds to the splitting of a multidimensional transfer equation

$$\frac{\partial f}{\partial t} + \vec{c} \cdot \frac{\partial f}{\partial x} = 0$$

into a sequence of one-dimensional finite-difference schemes.

The Boltzmann equation is known to imply a molecular chaos or a statical independence of particles.* The same premises are inherent in our model as in the Boltzmann equation but without the assumption of molecular chaos (statistial independence). In our model statistical dependence of the particles violates molecular chaos. It should be noted that the inherent statial independence rests upon theoretical and physical premises and does not depend upon the mesh dimension (it exists as $\Delta x \to 0$ as well).

---

* The molecular chaos hypothesis implies that particle velocities are statistically independent. (M.N. Kogan, "Rarefied Gas Dynamics," M., Nauka, 1967).

The numerical results of rarefied gas flow reveal that:

1) results of calculations with various numbers of particles in a cell (e.g. with N = 3 and N = 20) practically coincide;

2) these results are in good agreement with the solution of the Boltzmann equation (Cheremisin's and Rykov's data). Therefore, the violation of molecular chaos in the problems involved is small (though statical dependence exists, it is weakly manifested in rarefied gas problems, and apparently, it can be neglected here).

For the study of turbulence, statistical independence is of crucial significance and we expect that it will be manifested in this method when applied to turbulent flows.

5.2 Simulated Structure of a Shock Wave

The model was tested for the solution of a problem dealing with the structure of a normal shock wave in a gas consisting of elastic spheres in the range of Mach numbers M_∞ = 1.25 to 4.

Graphs of density $\tilde{n}(x)$, longitudinal temperature $\tilde{T}_{11}(x)$, transverse temperature $\tilde{T}_1(x)$ and static temperature $\tilde{T}(x)$ are shown in Figs. 17 and 18 for M = 2 and 3. The unit of length is the mean free path of molecules in the free stream flow. The value of $\Delta t/\Delta x$ was chosen to insure stability of the calculations. The average number of particles in cells corresponding to the oncoming flow is N_0 = 15 to 20 (M = 2) and N_0 = 12 (M = 3). A comparison is made in the figures with the density $\tilde{n}(x)$ and temperature $\tilde{T}(x)$ obtained by direct numerical integration of the Boltzmann equation [35,36] on a network Δx similar to the one used in our calculations (Δx = 0.2 to 0.3).

Finally, Figs. 19 and 20 show that the results of the calculations are

only weakly dependent upon the average number of particles N_0 in the cells for rarefied gas flows.

6. Numerical Investigation of Some Gas Dynamics Problems by Net-Characteristic Methods.

The manifold problems presently confronting computational mechanics are increasing in complexity, which in turn requires the improvement of earlier numerical methods and the creation of new ones. The properties that a numerical method is to be endowed with, from the view-point of modern developments, are so diverse that they are difficult to fully implement in one single method. In view of this, complexes of numerical methods based upon a unified approach should be available.

A large and important class of problems is described by multi-dimensional systems of equations of hyperbolic type. A fundamental concept underlying the construction of numerical approximations for such systems requires that their characteristic properties be taken into account in some form, i.e., it is essential to impart relevant features to the numerical methods of their solution as well. Finally, it is desirable to consider homogeneous schemes that enable calculations through discontinuities that may arise in the evolution of the solution, that allow for explicitly singling our some (principal) of the features and that adequately resolve their boundary conditions.

6.1 Investigation of Difference Schemes for a Model Equation

Positive type difference schemes, first introduced in [37], play an important role in the solution of equations of hyperbolic type. Using the method of indefinite coefficients and the characteristic properties of equations of hyperbolic type, one can write a rather large class of schemes of this kind and then perform a comparative analysis, in particular, with respect to the magnitude of "approximation viscosity" (see, e.g., [38]).

These schemes possess a number of indisputable advantages, the main ones are the absence of oscillations in the numerical simulation of non-smooth solutions, and the construction of efficient algorithms for the calculation of boundary points. However, since they are all of first-order accuracy, the utilization of even the best of the schemes [39,40] (having a minimal "approximation viscosity") requires in some cases a great number of grid points in the difference net and, consequently, a voluminous number of calculations. Some schemes of higher order accuracy can be constructed by a similar method in which difference approximations are treated as components of a linear space of indefinite coefficients.

The basic idea of the method is illustrated by the simple wave equation

$$v_t + \lambda v_x = 0, \lambda = \text{const.}, \quad \lambda > 0 \tag{25}$$

discretized in a pattern typical of explicit schemes comprising six points (Fig. 21)

$$(t^{n+1}, x_m)(t^n, x_{m-2}),\ldots,(t^n, x_{m+2}) , \tag{26}$$

Linear difference schemes written for the pattern (26) in the following form

$$v_m^{n+1} = \sum_{\mu,\nu} \alpha_\mu^\nu v_{m+\mu}^{n+\nu} = \sum_{\mu=-2}^{2} \alpha_\mu v_{m+\mu}^n \tag{27}$$

when substituted into (25) yield

$$\begin{aligned} &\sum_{\mu,\nu} (\mu - \nu\sigma)\, \alpha_\mu^\nu = -\sigma \\ &\sum_{\mu,\nu} \alpha_\mu^\nu = 1, \ \sigma = \lambda\tau/h \geq 0 , \end{aligned} \tag{28}$$

where coefficients α_{-1} and α_1 are excluded.

Any point in the space of the coefficients that remain indeterminate $\alpha = \{\alpha_{-2}, \alpha_0, \alpha_2\}$ (figs. 22a,b) gives rise to a difference scheme of first-order accuracy for eq. (25); when this point is inclosed by polyhedrons

$A_1A_3,\ldots,A_6$ with $0 \leq \sigma \leq 1$ (fig. 22a) or $A_2A_3A_4A_6$ with $1 < \sigma \leq 2$ (fig. 22b) it gives rise to difference schemes of positive approximation for which all coefficients

$$\alpha_\mu^\nu \geq 0 \ . \tag{29}$$

Points A_1 with $0 \leq \sigma \leq 1$ (scheme [39]) and A_2 with $1 < \sigma \leq 2$ correspond to difference schemes with the least "approximation viscosity", i.e., with the smallest value of the coefficient of v_{xx} in the first differential approximation of (27) [38].

Plane $B_1,\ldots,B_9$ (fig. 22)

$$\sum_{\mu,\nu} (\mu - \nu\sigma)^2 \alpha_\mu^\nu = \sigma^2, \qquad \text{or} \qquad \alpha_o = 3(\alpha_{-2} + \alpha_2) + 1 - \sigma^2 \tag{30}$$

for the pattern (26) constitutes a two-parameter family of difference schemes of second-order accuracy for the solutions of (25). In figs. 22a,b the boundaries of the region of stable schemes with an approximation order higher than the first are shown by ticked lines on plane (30). It is seen that with $0 \leq \sigma \leq 2$ this region is not empty. It is shown in [41] that there are no difference schemes of the form (27) having a second order approximation (a higher order accuracy as well, see [38]) which satisfies the constraints of eq. (29), i.e., plane (30) does not intersect a closed polyhedron (28), (29).

A straight line $C_1.....C_5$ being an intersection line of plane (30) and the plane

$$\sum_{\mu\ \nu} (\alpha - \nu\sigma)^3 \alpha_\mu^\nu = -\sigma^3 \ , \tag{31}$$

incorporates a one-parameter family of schemes of third-order accuracy. With $0 \leq \sigma \leq 1$ the segment C_1C_6 (fig. 22a) contains stable schemes of third-order accuracy. Point C_1 on the pattern given is the only difference

scheme of fourth-order accuracy. The familiar Lax-Wendroff scheme is indicated by point B_5 in figs. 22a,b.

6.2 Construction of Positive-Type Difference Approximations.

Evidently, various kinds of oscillations of nonsmooth solutions that are observed in familiar difference schemes with an approximation order higher than the first, and that are not present in schemes of positive type approximation, are due to the fact that some of the coefficients α_μ^ν in difference expressions of the form (27) are negative for schemes of higher order accuracy. It is natural to suppose that the behavior of a particular scheme for nonsmooth solutions (the amplitude and character of oscillations) is determined by the distance of a point (corresponding to this scheme in the space of indeterminate coefficients) from the region of difference schemes with positive approximation (from polyhedrons $A_1A_3\ldots A_6$ (fig. 22a), $A_2A_3A_4A_6$ (fig. 22b) etc.). From this observation, it is proposed that the "non-monotonicity" of difference schemes be characterized by the value

$$\gamma = |\alpha - \alpha_A| \ , \tag{32}$$

where $\alpha\{\alpha_\mu^\nu\}$ is the set of coefficients in eq. (27) corresponding to the difference scheme in question (of approximation order higher than the first situated on plane (30)), and α_A is the set of coefficients in eq. (27) corresponding to the vertex of the polyhedren prescribed by eqs. (28), (29) which describe difference schemes of first-order accuracy of positive type approximation (point A_1 in fig. 22a with $0 \leq \sigma \leq 1$ and point A_2 in fig. 22 with $1 \leq \sigma \leq 2$ etc.). That is, schemes of first-order accuracy should be constructed on three-point patterns incorporating the point (t^{n+1}, x_m) that is to be calculated and two nodes of the difference molecule along t^n which

just brackets the characteristics $dx = \lambda dt$ (e.g., x_{m-2}, x_{m-1} of fig. 21).

For difference schemes for the solution of (25) of second-order accuracy, the coefficients α_μ^ν are found by a conventional geometric construction in the α-space ($\alpha = \{\alpha_{-2}, \alpha_0, \alpha_2\}$) of the point of intersection with plane (30) of the normal drawn from point A. With $0 \leq \sigma \leq 1$ ($\alpha_A = \{0, 1-\sigma, 0\}$) this procedure results in point B_6 in fig. 22a, a difference scheme of second-order accuracy. With $1 \leq \sigma \leq 2$ such a scheme corresponds to point B_9 in fig. 22b. ($\alpha_A = \{\sigma - 1, 0, 0\}$).

The difference scheme of third-order accuracy with the smallest value of γ which is stable for $0 \leq \sigma \leq 1$ is found by constructing the point of intersection of the normal drawn from point $\alpha_A = \{0, 1-\sigma, 0\}$ with the straight line ((30), (31)), point C_3 in Fig. 22a.

The calculation of the simplest modelling problems reveals that difference schemes of second and third-order accuracy constructed in this manner have the shortest amplitude of oscillations with fast damping as compared to other schemes.

Bearing in mind that eq. (25) is, in essence, an ordinary differential equation along the characteristic $dx = \lambda dt$

$$\frac{dv}{dt} = 0, \quad \frac{d}{dt} = \frac{\partial}{\partial t} + \lambda \cdot \frac{\partial}{\partial x}$$

and, consequently, at point (t^{n+1}, x_m) the exact value is

$$v_m^{n+1} = v(t^m, \tilde{x}) \ , \quad \tilde{x} = x_m - \lambda\tau \ ,$$

so that the difference expressions in the right-hand part of (27) are essentially interpolation formulas for calculating $v(t^n, \tilde{x})$. From this viewpoint the right-hand part of eq. (27) for schemes possessing the smallest value of γ may be treated as interpolation polynomials of the second and

third-order for the function $v(t^n,\tilde{x})$; these polynomials differ from a piecewise-linear interpolation relevant to difference schemes of first--order accuracy with positive approximation. A more detailed description of the approach in hand including "implicit" difference molecules will be given in a forthcoming publication.

6.3 Positive-Type Difference Schemes for Model Equations

The construction of difference schemes of sections 6.1 and 6.2 is realized by a separate compatibility condition along characteristics $dx=\lambda_i dt$ of a one-dimensional system of equations of hyperbolic type

$$U_t + AU_x = f \quad , \quad A = \Omega^{-1}\Lambda\Omega \quad , \tag{33}$$

which, in a conventional way, is reduced to canonical form

$$w_i U_t + \lambda_i w_i U_x = w_i f \ , \ i = 1,\ldots,I \ . \tag{34}$$

Here $U = \{U_1,\ldots,U_I\}$ is the vector of unknown functions; $f = \{f_1,\ldots,f_I\}$ - is a vector-column of right-hand parts; $\Lambda = \{\lambda_i\}$ is a diagonal matrix from eigenvalues of matrix A; $\Omega = \{w_i\}$ is a nonsingular matrix whose lines are linear-independent eigenvectors w_i of the matrix A.

If matrix A has fixed components and $f = 0$, difference schemes (27) are generalized, in an obvious manner, for the case of system (9)

$$U_m^{n+1} = \sum_{\mu,\nu} D_\mu^\nu \, U_{m+\mu}^{n+\nu} \cdot D_\mu^\nu = \Omega^{-1} A_\mu^\nu \Omega \ ,$$

where $A_\mu^\nu = \{(\alpha_\mu^\nu)_i\}$ are diagonal matrices. The general quasilinear case of system (33) ($A = A(t,x,v)$, $f = f(t,x,v)$) requires the development of a proper method of integration of "ordinary" differential equations (34) that takes into account the dependence of λ_i, w_i, f upon the unknown solution v and independent variables t, x. Different approaches may be used for this purpose. One example, intended for the construction of explicit difference schemes using the pattern of type (26), is the Runge-Kutta method applied in [43]

and in a number of subsequent papers (see, e.g., [44]).

In [43] for a system expressed in divergence form

$$U_t + F_x(t,x,U) = \phi \ , \tag{35}$$

on the pattern (26) a one-parameter family of difference schemes of third-order accuracy was constructed

$$U^{n+\alpha}_{m+\frac{1}{2}} = (U^n_m + U^n_{m+1})/2 - \alpha\tau(F^n_m - F^n_m)/h + \alpha\tau(\phi^n_{m+1} + \phi^n_m)/2 \ , \tag{36}$$

$$U^{n+\beta}_m = U^n_m - \beta\tau(F^{n+\alpha}_{m+\frac{1}{2}} - F^{n+1}_{m-\frac{1}{2}})/h + \beta\tau(\phi^{n+\alpha}_{m+\frac{1}{2}} + \phi^{n+\alpha}_{m-\frac{1}{2}})/2 \ , \tag{37}$$

$$\begin{aligned} U^{n+1}_m = U^n_m + \frac{3\tau}{4}\left[-\frac{(F^{n+\beta}_{m+1} - F^{n+\beta}_{m-1})}{2h} + \phi^{n+\beta}_m\right] + \frac{\tau}{4}\left[-\frac{(F^n_{m+1} - F^n_{m-1})}{2h} + \phi^n_m\right] + \\ + \tau\,(F^n_{m-2} - 2F^n_{m+1} + 2F^n_{m-1} - F^n_{m-2})/12h + g(U^n_{m-2} - 4U^n_{m-1} + 6U^n_m - 4U^n_{m+2} + U^n_{m+2}) \ , \end{aligned} \tag{38}$$

$$\alpha = 1/3 \ , \quad \beta = 2/3.$$

It was also shown there that to insure stability of these schemes the value of the parameter g is subject to the condition:

$$-1/8 \le g \le \sigma_*^2(\sigma_*^2 - 4)/24 \ , \quad \sigma_* = \tau \max_{m,i}|\lambda_i|/h. \tag{39}$$

According to the analysis carried out in sec. 6.1,2 for linear equations, it is preferable to choose a matrix

$$\begin{aligned} &\Omega^{-1} \cdot G\Omega \ , \quad G = \{g_i\} \ , \quad \Omega = \{w_i\} \ , \\ &g_i = |\sigma_i| \cdot (5|\sigma_i| - 24)/152 \ , \quad \sigma_i = \lambda_i\tau/h, \quad i = 1,\ldots,I. \end{aligned} \tag{40}$$

instead of a scalar factor in the last term of (38) which is the same for all characteristics. In equation (39) and (40) λ_i are the eigenvalues of the matrix $A = \partial F/\partial u$, Ω is a matrix derived above from the eigenvectors, and G is a diagonal matrix. The modification just cited of the scheme (36-38) for a linear case is the scheme discussed in section 6.2 corresponding to the smallest value of γ. We should also note that the last term in (38), modified in accordance with (40), is more conveniently written in divergence form

$$(\Omega^{-1}G\Omega)^n_{m+\frac{1}{2}} \cdot (-U^n_{m+1}+3U^n_m-3U^n_{m+1}+U^n_{m+2}) -$$
$$-(\Omega^{-1}G\Omega)^n_{m-\frac{1}{2}} \cdot (-U^n_{m-2}+3U^n_{m-1}-3U^n_m+U^n_{m+1}) \qquad (41)$$

On the same pattern of (26) there can be generalized for the case of quasilinear systems (35), difference schemes of second-order accuracy which are "closer" to schemes with positive approximation, for example, in the form of a two-step system with a predictor - the Lax scheme with $\alpha = 0.5$ in (36) and a corrector

$$U^{n+1}_m = (\Omega^{-1}A_2\Omega)^n_{m+\frac{1}{2}} (-U^n_{m-1} + 3U^n_m - 3U^n_{m+1} + U^n_{m+2}) -$$
$$- (\Omega^{-1}A_2\Omega)^n_{m-\frac{1}{2}} (U^n_{m-2} + 3U^n_{m+1} - 3U^n_m + U^n_{m+1}) + \qquad (42)$$
$$+ U^n_m - \tau(F^{n+\frac{1}{2}}_{m+\frac{1}{2}} - F^{n+\frac{1}{2}}_{m-\frac{1}{2}})/h + \tau(\phi^{n+\frac{1}{2}}_{m+\frac{1}{2}} + \phi^{n+\frac{1}{2}}_{m-\frac{1}{2}})/2$$

which is stable providing

$$\sigma_* = \tau \max_{m,i} |\lambda_i|/h \leq 2. \qquad (43)$$

Here $A = \{(\alpha_{-2})_i\}$, $A_2 = \{(\alpha_2)_i\}$ are diagonal matrices with elements

$$\left.\begin{aligned}(\alpha_2)_i &= 3(1 - \sigma_i)(2 - \sigma_i)/19,\\ (\alpha_{-2})_i &= (\alpha_{-2})_i - (1 - \sigma_i)\end{aligned}\right\} \text{ for } \quad 1 < \sigma_i \leq 2$$

$$\left.\begin{aligned}(\alpha_{-2})_i &= 3(1 + \sigma_i)(2 + \sigma_i)/19,\\ (\alpha_2)_i &= (\alpha_{-2})_i - (1 + \sigma_i)\end{aligned}\right\} \text{ for } \quad -2 \leq \sigma_i < -1, \qquad (44)$$

$$(\alpha_2)_i = (\alpha_{-2})_i = -3|\sigma_i| \ (-1 - |\sigma_i|/19 \quad \text{for } |\sigma_i| \leq 1.$$

It is seen that satisfying the more restrictive condition of $\sigma_* \leq 1$, rather than (43), the scheme of (36), (42), and (44) is conservative. The last three terms in equation (42) coincide with the familiar Lax-Wendroff scheme [42] and can be replaced by other modifications of analogous schemes [45].

As an example, in fig. 23a, results for $t/\tau = 52$ of numerical solutions, using the second-order accurate scheme (36), (42), (44) (scheme II), the Lax-Wendroff scheme [42], and the MacCormak scheme [45], are compared with the exact solution (dashed lines) for a problem concerned with one-dimensional wave motion in gas resulting from initial conditions: $v(0,x) = 0$, $\rho(0,x) = p(0,x) = 2$ for $x \leq 0$; $\rho(0,x) = p(0,x)$ with $x > 0$. In fig. 23b a similar comparison is given for the scheme (36)-(38) with ($\sigma_* = 1$) choosing g_i from (40) (scheme III) and $g_i = \sigma_*^2(\sigma_*^2 - 4)/24 = -1/8$. In the same figure a scheme of first-order accuracy with positive approximation [46] (scheme I) is compared with the exact solution and schemes of third-order accuracy.

In this problem, as well as in the linear case, one observes the improvement of "oscillation" properties in schemes II, III as compared to other schemes of second and third-order accuracy. Note that scheme I as far as its accuracy is concerned is quite comparable with schemes II, III in the calculation of shock waves; however, it requires a very fine difference net for calculations through contact discontinuities.

6.4 Applications to Gasdynamics Problems

Without elaborating here upon the generalization of the difference schemes described to multidimensional cases it should only be noted that, for schemes of first-order accuracy with positive approximation (27), (28), the construction procedures are performed rather formally (see, e.g., [39,46,47]). For difference schemes of higher-order accuracy there also exist various efficient approaches described in detail in scientific publications.

In the past years systematic investigations have been conducted on the aerodynamics of bodies of complex geometry, on numerical modelling of problems in plasma physics, and on dynamic problems in the theory of elasticity

utilizing some of the difference schemes discussed above. The prominent features in such problems are the complex structure of the unknown solution, the presence of regions with large gradients, and discontinuous functions.

Stable schemes of first-order accuracy [47] prove to be sufficiently effective for the numerical solution of problems that involve a comparatively small number of discontinuity surfaces; they can be explicitly defined formulating on them appropriate boundary conditions.

As an example, in fig. 24a are shown the stationary bow shock patterns in the plane of symmetry of a supersonic three-dimensional inviscid flow of a thermally nonconducting gas (adiabatic index of k = 1.4) around a spherically blunted cone of $\theta_k = 10^o$ half-angle which has a segmentally capped base ($\theta_c = 35^o$). The overall length of the body is equal to 5.5 radii of the spherical nose blunting. The Mach number of the incoming flow was M=2, with the angle of attack varied from 0 to 180^o. Fig. 24b presents the corresponding pressure distributions along this body. Other problems of three--dimensional supersonic flow of a radiating gas around blunt bodies, solved by means of the numerical method of [47] under the assumption of thermochemical equilibrium, are described in detail in [48-52].

Solutions to problems containing singularities (discontinuities) within the integration region are obtained (with acceptable accuracy) without singling them out explicitly by the introduction of conservative elements (see, e.g., [38,46]) in the difference scheme of [47]. A number of one- and two-dimensional problems involving the interaction of laser light with matter are considered by this scheme. As a typical example of this kind (taken from [46]) fig. 25 presents at a time instant $t = 10^{-10}$ sec., appropriate to the termination of the impulse, the isochores ρ/ρ_o = const. (fig. 25a) and isotherms in Kev (the electronic temperature Te = const, solid

curves, and the ionic plasma temperature Ti = const. - dashed curves, fig. 25b) in the interaction of a symmetrical impulse of laser light of energy E = 300j with a spherical envelope of variable radius. The initial disturbances of the envelope are located at its hali-radius and the following physical processes are taken into account; the absorption of outer laser radiation, nonlinear electronic thermal conduction, and electron-ion collisional relaxation. The terms in the energy equations for electronic and ion components related to thermal conduction and energy exchange between the components are approximated in an implicit way. The direct application of the schemes of [47] for the solution of similar problems resulted in a significant violation of the integral balance of mass, momentum and energy, so that the solution in the vicinity of a nonstationary shock wave moving along a cold background is quite unsatisfactory.

The last example of the net characteristic methods is shown in Fig. 26, an instantaneous picture of the distribution of components σ_{yy}, σ_{xy}, σ_{xx} of a stress tensor in an elastic layer of finite thickness at the instant $t = t_* = 0.029$. They are produced by the nonstationary loading, P, on part of the upper boundary of the elastic layer which is supported on a perfectly plane rigid base. Boundary conditions in this problem are given as follows: on the portion AB of the upper boundary,

$$v_y(t,x,1) = -\frac{1}{m_o}\int_o^t dt[P+2\int_A^B \sigma_{yy}(t,x,1)dx] \quad \text{see the inset of Fig. 26c,}$$

$$\sigma_{xy}(t,x,1) = 0;$$

on the other portion of the upper boundary,

$$\sigma_{yy}(t,x,1) = \sigma_{xy}(t,x,1) = 0,$$

on the lower boundary, y = .5,

$$v_y(t,x,0.5) = \sigma_{xy}(t,x,0.5) = 0.$$

AO is a plane of symmetry and m_o, the mass density of the elastic layer, is

a constant.

In conclusion, the author would like to express his sincere gratitude to V.V. Demchenko and I.B. Petrov who were helpful in obtaining the numerical solutions of some of the problems described.

REFERENCES

1. A.A. Dorodynitsyn, "On One Method of the Equation Solution of the Laminar Boundary Layer Equation," Zh. Prikl. Mekhan. i Tekhn. Fiz., Vol. 1, No. 3, 1960, pp. 111-118.

2. O.M. Belotserkovskii, "A Flow With a Detached Shock Wave Around A Circular Cylinder," Dokl. AN SSSR, Vol. 113, No. 3, 1957, pp. 509-512.

3. O.M. Belotserkovskii, "A Flow With a Detached Shock Wave Around a Symmetrical Profile," Sov. J. Appl. Math & Mech.*, Vol. 22, No. 2, 1958, pp. 279-296.

4. O.M. Belotserkovskii, P.I. Chushkin, "A Numerical Method of Intergral Relation," USSR J. Comp. Math & Math Phys.**, Vol. 2, No. 5, 1962, pp. 825-858.

5. O.M. Belotserkovskii, A. Bulekbayev, V.G. Grudnitskii, "Algorithms for Schemes of the Method of Integral Relations Applied to the Calculations of Mixed Gas Flow," USSR J. Comp. Math & Math Phys., Vol. 6, No. 6, 1966, pp. 162-184.

6. O.M. Belotserkovskii, "Flow Past Blunt Bodies in Supersonic Flow; Theoretical and Experimental Results," Trudy Vych. Ts. AN SSSR, Computing Center AN SSSR, Moscow, 1966 (1st edition, 1967 (2nd edition, revised and extended), NASA Technical Translation, F-453, 1967.

7. P.I. Chushkin, "Blunt Bodies of Simple Form in Supersonis Gas Flow," Sov. J. Appl. Math & Mech., Vol. 24, No. 5, 1960, pp. 1397-1403.

8. P.I. Chushkin, "Method of Characteristics for Three-Dimensional Supersonic Flow," Trudy Vych. Ts. AN SSSR, Moscow, 1968.

9. K.M. Magomedov, A.S. Kholodov, "On the Construction of Difference Schemes for Equations of Hyperbolic Type Based on Characteristic Coordinates," USSR J. Comp. Math & Math Phys., Vol. 9, No. 2, 1969, pp. 158-175.

10. O.M. Belotserkovskii, Numerical Investigation of Modern Problems in Gas Dynamics, Izd. "Nauka", Moscow, 1974.

11. F.H. Harlow, "The Particle-in-Cell Computing Method for Fluid Dynamics," Methods in Computational Physics, Vol. 3, Berni Alder, Sidney Fernbach, Manuel Rotenberg, eds., Academic Press, N.Y., 1964.

---

* Pergamon Press translation of Prikl. Mat. i Mekhan.

** Pergamon Press translation of Zh. Vychisl. Matem. i Matem. Fiz.

12. M. Rich, "A Method for Eulerian Fluid Dynamics, Los Alamos Scientific Laboratory, New Mexico, LAMS-2826, 1963.

13. C.W. Hirt, "Heuristic Stability Theory for Finite-Difference Equations," J. Comp. Phys., Vol. 2, No. 4, 1968, pp. 339-355.

14. O.M. Belotserkovskii, Yu. M. Davidov, "The Use of Unsteady Methods of 'Large Particle' for Problems of External Aerodynamics," Preprint Vych. Ts. AN SSSR, 1970, 85 p.

15. O.M. Belotserkovskii, Yu. M. Davidov, "A Non-Stationary 'Coarse Particle' Method for Gas Dynamical Computations," USSR J. Comp. Math & Math Phys., Vol. 11. No. 1, 1971, pp. 242-271.

16. V.A. Gushchin, V.V. Shchennikov, "On One Numerical Method of the Solution of the Navier-Stokes Equation," USSR J. Comp. Math & Math Phys., Vol. 14, No. 2, 1974, pp. 242-250.

17. O.M. Belotserkovskii, V.A. Gushchin, V.V. Shchennikov, "Method of Splitting Applied to the Solution of Problems of Viscous Incompressible Fluid Dynamics," USSR J. Comp. Math & Math Phys., Vol. 15, No. 1, 1975, pp. 190-200.

18. O.M. Belotserkovskii, L.I. Severinov, "The Conservative 'Flow' Method and the Calculation of the Flow of a Viscous Heat-Conducting Gas Past a Body of Finite Size," USSR J. Comp. Math & Math Phys., Vol. 13, No. 2, 1973, pp. 141-156.

19. O.M. Belotserkovskii, E.G. Shifrin, "Transonic Flow Behind a Detached Shock-Wave," USSR J. Comp. Math & Math Phys., Vol. 9, No. 4, 1969, pp. 230-260.

20. O.M. Belotserkovskii, Yu. M. Davidov, "Computation of Transonic 'Supercritical' Flows by the 'Coarse Particle' Method," USSR J. Comp. Math & Math Phys., Vol. 13, No. 1, 1973, pp. 187-216.

21. V.E. Yanitsky, "Use of Poisson's Stochastic Process to Calculate the Collision Relaxation of Non-Equilibrium Gas," USSR J. Comp. Math & Math Phys., Vol. 13, No. 2, 1973, pp. 310-317.

22. V.E. Yanitsky, "Application of Random Motion Processes for Modelling Free Molecular Gas Motion," USSR J. Comp. Math & Math Phys., Vol. 14, No. 1, 1974, pp. 264-267.

23. O.M. Belotserkovskii, V.E. Yanitsky, "Statistical 'Particle-in Cell' Method for the Solution of the Problem of Rarefied Gas Dynamics," USSR J. Comp. Math & Math Phys., Vol. 15, No. 5, 1975, pp. 101-114 (part I) and No. 6, 1975, pp. 184-198 (part II).

24. N.N. Yanenko, Y.I. Shokin, "On the First Differential Approximation of Difference Schemes for Hyperbolic Sets of Equations," Sibirskii Mat. Zh., Vol. 10, No. 5, 1969, pp. 1173-1187.

25. R.A. Gentry, R.E. Martin, J. Daly, "An Eulerian Differencing Method for Unsteady Compressible Flow Problems," J. Comp. Phys., Vol. 1, 1966, pp. 87-118.

26. G.P. Wood and P.B. Gooderum, "Investigation with an Interferometer of the Flow Around a Circular-Arc Airfoil at Mach Numbers Between 0.6 and 0.9", Natl. Advisory Comm. Aeron. (NACA) Tech. Note No. 2801, U.S. Govt. Printing Office, Washington, D.C., October 1952.

27. A.A. Amsden, F.H. Harlow, "The SMAC Method," Los Alamos Scientific Laboratories, New Mexico, Rept. LA-4370, 1970.

28. C.R. Easton, "Homogeneous Boundary Conditions for Pressure in MAC Method," J. Comp. Phys. Vol. 9, No. 2, 1972, pp. 375-379.

29. V.V. Gushchin, V.V. Shchennikov, "Solution of Problems of Viscous Incompressible Fluid Dynamics by the Method of Splitting," Sb. Vych. Mat. i Mat. Fiz., No. 2, 1974.

30. A.V. Babakov, O.M. Belotserkovskii, L.I. Severinov, "Numerical Investigation of a Viscous Heat-Conducting Gas Flow Past a Blunt Body of Finite Size," Izv. Ak. Nauk SSSR, Mech. jidkosti i gaza, No. 3, 1975, pp. 112-123.

31. O.M. Belotserkovskii, "Calculation of the Flow Around Axially Symmetric Bodies with a Detached Shock Wave," Preprint Comp. Center Ak. Nauk SSSR, 1961.

32. G.A. Bird, "The Velocity Distribution Function Within a Shock Wave," J. Fluid Mech., Vol. 30, Pt. 3, 1967, pp. 479-487.

33. G.A. Bird, "Direct Simulation and the Boltzmann Equation," Phys. Fluid, Vol. 13, No. 11, 1970, pp. 2677-2681.

34. M. Kats, Probability and Related Topics in Physical Sciences, Izd. "Mir", Moscow, 1965.

35. F.G. Cheremisin, "Numerical Solution of the Boltzmann Kinetic Equation for One-Dimensional Stationary Gas Motion," USSR J. Comp. Math & Math Phys., Vol. 10, No. 3, 1970, pp. 125-137.

36. V.A. Rikov, "On Averaging the Boltzmann Kinetic Equation with Respect to a Transverse Velocity for the Case of One-Dimensional Gas Motion," Izv. Ak. Nauk SSSR, Mech. jidkosti i gaza, No. 4, 1969, pp. 120-127.

37. K.O. Fridrichs, "Symmetric Hyperbolic Linear Differential Equations," Comm. Pure and Appl. Math, Vol. 7, No. 2, 1954, pp. 345-392.

38. A.S. Kholodov, "On the Construction of Difference Schemes of Positive Approximation for Equations of Hyperbolic Type," Zh. Vych. Mat i Mat Fiz., Vol. 18, No. 6, 1978, pp. 1476-1492.

39. R. Courant, E. Isacson, M. Rees, "On the Solution of Nonlinear Hyperbolic Differential Equations by Finite Differences," Comm. Pure and Appl. Math., Vol. 5, No. 5, 1952, pp. 243-254.

40. H.B. Keller, B. Wendroff, "On the Formulation and Analysis of Numerical Methods for Time Dependent Transport Equations," Comm. Pure and Appl. Math, Vol. 10, No. 4, 1957, pp. 567-582.

41. S.K. Godunov, "Difference Methods of Numerical Calculation of Discontinuous Solutions of Equations of Hydrodynamics," Matem. Sbornik, Vol. 47, No. 3, 1959, pp. 271-306.

42. P.D. Lax, B. Wendroff, "Systems of Conservation Laws," Comm. Pure and Appl. Math., Vol. 13, No. 2, 1960, pp. 217-237.

43. V.V. Rusanov, "Difference Schemes of Third Order Accuracy for a Swept Through Calculation of Discontinuous Solutions," Dokl. AN SSSR, Vol. 180, No. 6, 1968, pp. 1303-1305.

44. V.B. Balakin, "Methods of the Runge-Kutta Type for Gas Dynamics," USSR J. Comp. Math & Math Phys., Vol. 10, No. 6, 1970, pp. 208-216.

45. R.W. MacCormack, "The Effect of Viscosity in Hypervelocity Impact Cratering," AIAA Paper No. 69-354, Cincinnati, Ohio, 1969.

46. O.M. Belotserkovskii, V.V. Demchenko, V.I. Kosarev, A.S. Kholodov, "Numerical Modelling of Certain Problems of Laser Imploded Envelopes," Zh. Vych. Mat. i Mat. Fiz., Vol. 18, No. 2, 1978, pp. 420-444.

47. K.M. Magomedov, A.S. Kholodov, "The Construction of Difference Schemes for Hyperbolic Equations," USSR J. Comp. Math & Math Phys., Vol. 9, No. 2, 1969, pp. 158-175.

48. O.M. Belotserkovskii, ed., Numerical Investigation of Modern Gas Dynamics Problems, M. "Nauka", 1974.

49. O.M. Belotserkovskii, S.D. Osetrova, V.N. Fomin, A.S. Kholodov, "Hypersonic Flow of a Radiation Gas Over Blunt Bodies," USSR J. Comp. Math & Math Phys., Vol. 14, No. 4, 1974, pp. 168-179.

50. V.S. Kostrykin, V.N. Fomin, A.S. Kholodov, "Three-Dimensional Radiating Flow Around Blunted Cones and Ellipsoids of Revolution," USSR J. Comp. Math & Math Phys., Vol. 16, No. 2, 1976, pp. 166-174.

51. A.V. Krasilinikov, A.N. Nikulin, A.S. Kholodov, "Numerical Solution of the Problem of a Stream Impacting Against an Obstacle," Izv. Ak. Nauk SSSR Mekh. zhidk. i gaza, No. 5, 1975, pp. 179-181.

52. O.M. Belotserkovskii, L.I. Turchak, A.S. Kholodov, "Longitudinal Oscillation of Bodies of Revolution in Supersonic Flow," Izv. Ak. Nauk SSSR, Mekh. zhidk. i gaza, No. 5, 1975, pp. 110-115.

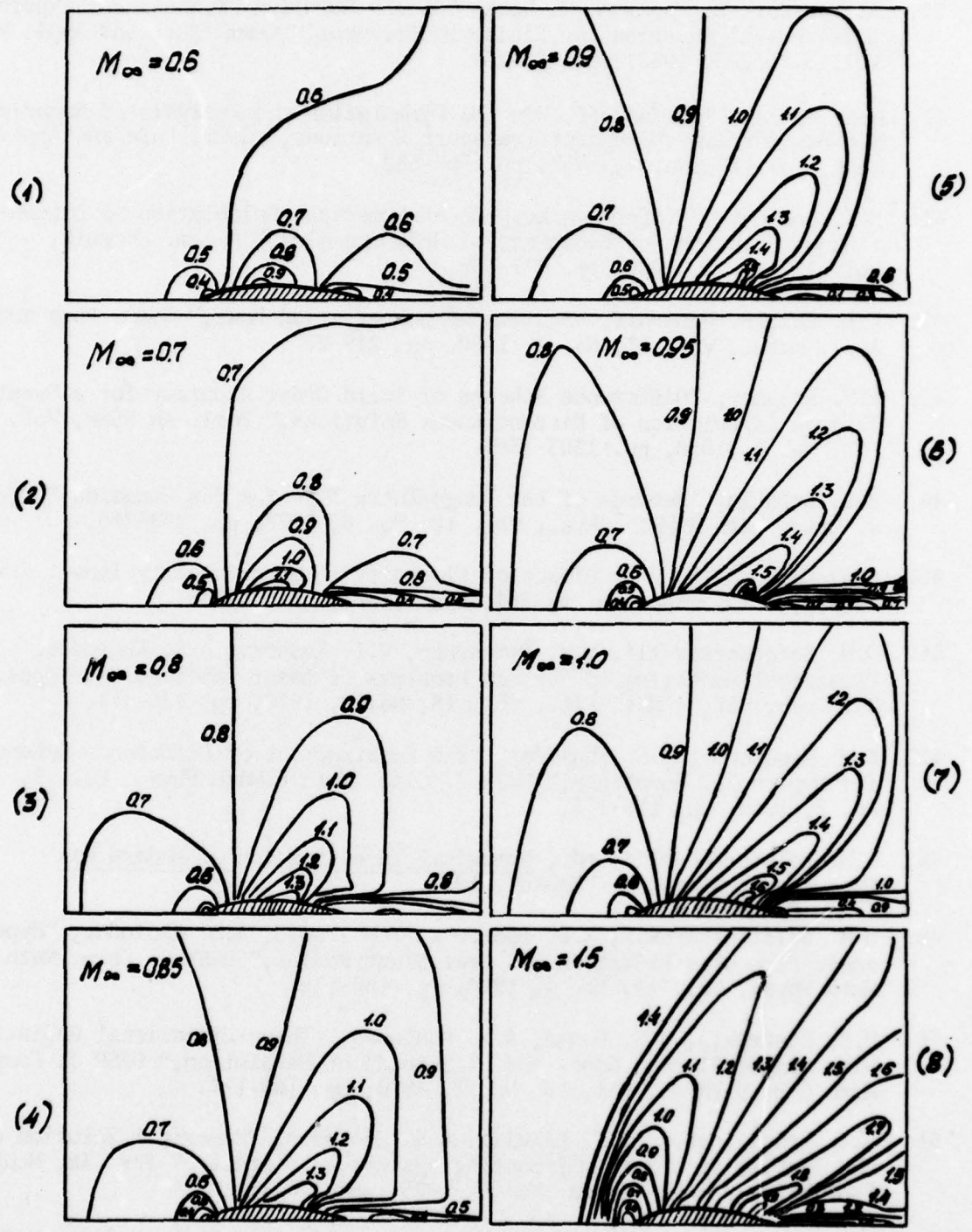

Fig. 1 Lines of constant Mach number (isotachs) in transonic flow past a two-dimension 24 per cent circular arc profile; critical Mach number, $M_\infty^* = 0.65$.

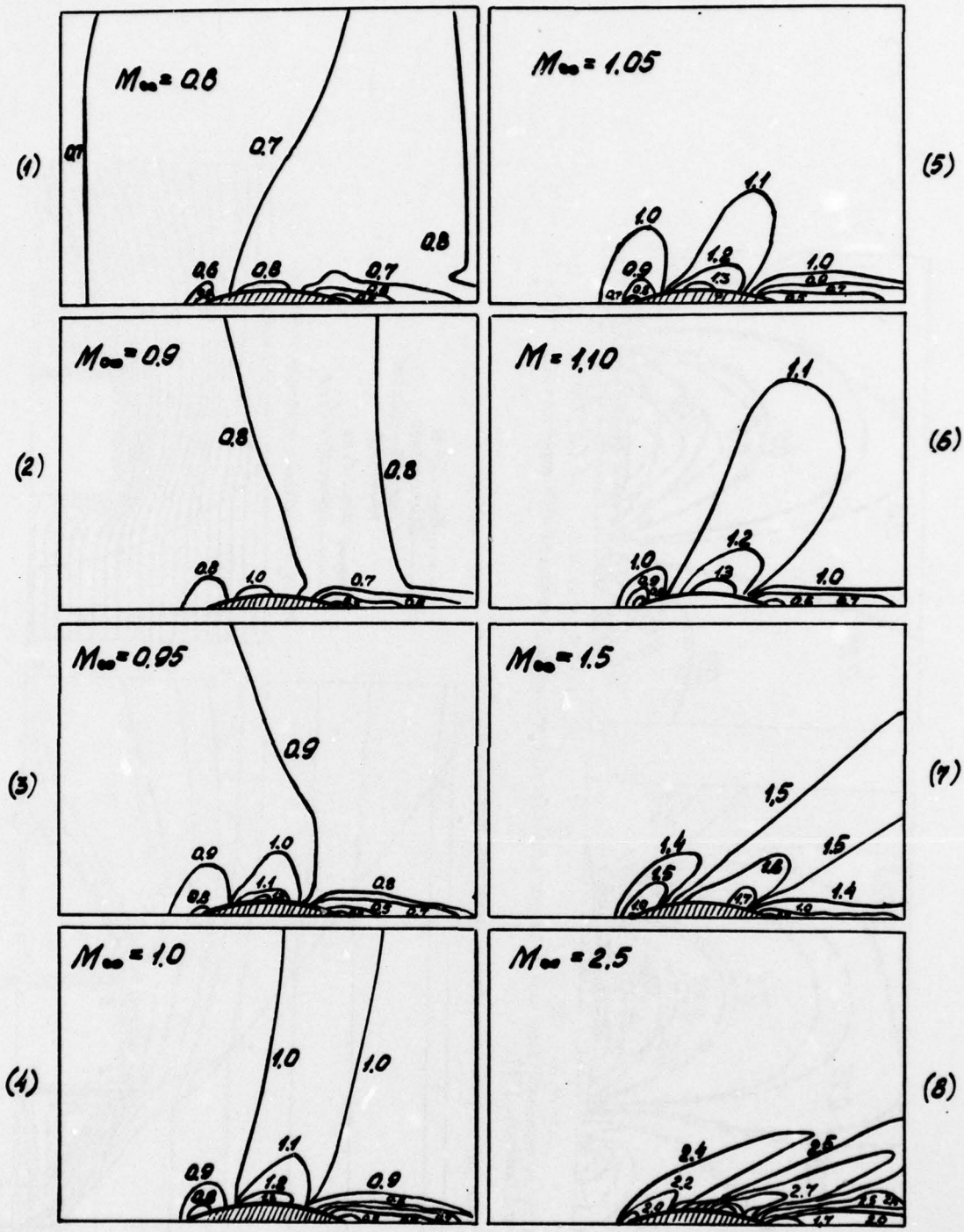

Fig. 2 Isotachs in transonic flow past a 24 per cent axisymmetric body (generated by revolution of a circular arc profile); critical Mach number, $M_\infty^* = 0.86$.

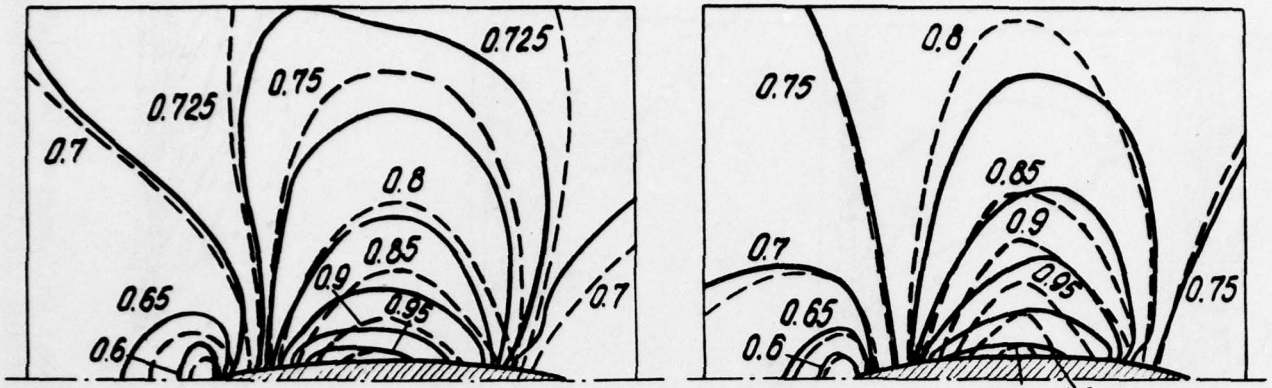

(a) M = 0.725 (b) M_∞ = 0.761

Fig. 3 Isotachs in transonic flow past a 12 per cent circular arc airfoil compared with experimental results (----) of Wood and Gooderum [26].

(a) $M_\infty = 3.5$, sonic jet on body axis, facing upstream, $M_C = 1.0$, $\rho_C = 2.9$

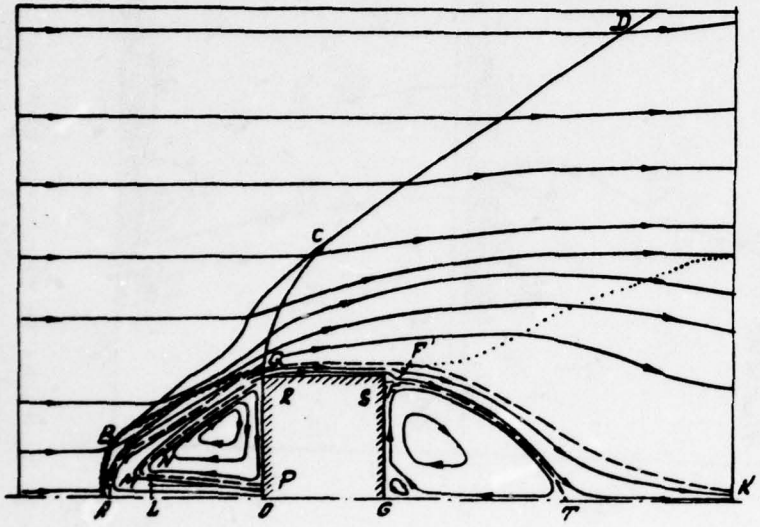

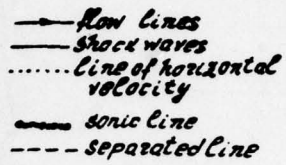

(b) $M_\infty = 2$, without upstream injection.

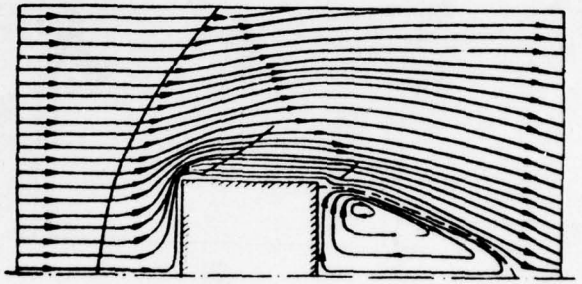

Fig. 4 Supersonic flow patterns around a thick circular disk.

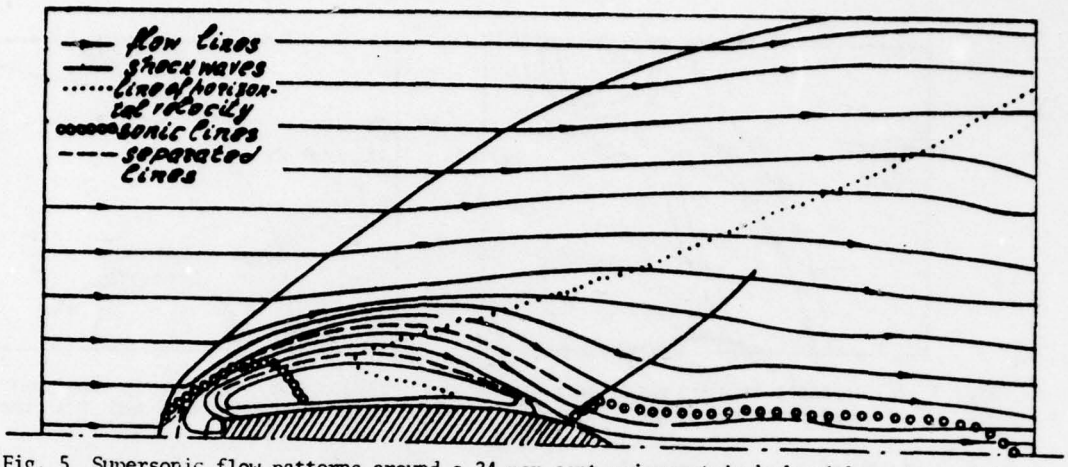

Fig. 5 Supersonic flow patterns around a 24 per cent axisymmetric body with upstream injection $M_\infty = 3.5$, $M_c = 1.0$ ($u_c = -1.0$, $v_c = 0$), $\rho_c = 2.9$.

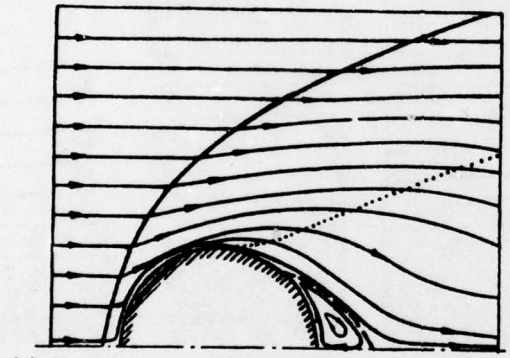

(a) $M_\infty = 3.5$, $M_c = 0$ (without upstream injection).

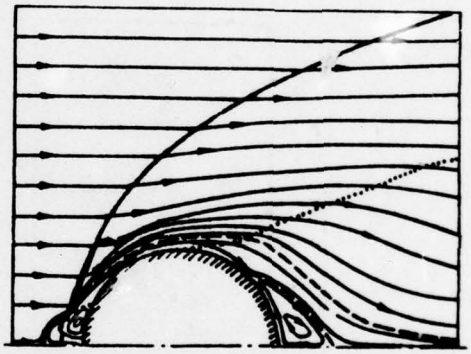

(b) $M_\infty = 3.5$, $M_c = 1$ ($u_c = -1.0$, $v_c = 0$), $\rho_c = 2.9$, sonic jet on body axis, facing upstream.

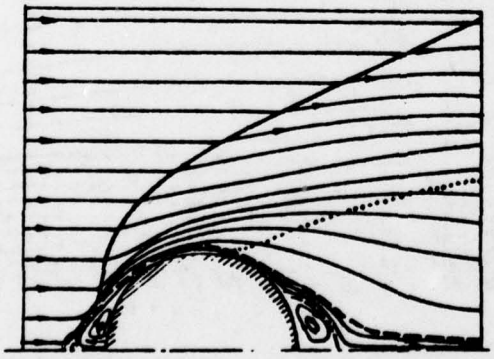

(a) $M_\infty = 6$, $M_c = 1$, $\rho_c = 2.9$

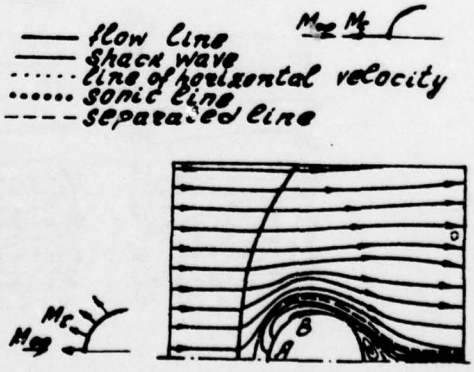

(d) injection with $M_c = 0.5$, distributed over surface A to B.

Fig. 6 Supersonic flow patterns around a sphere.

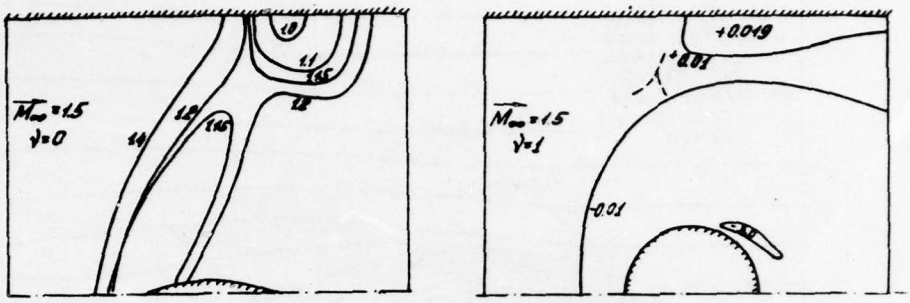

Fig. 7 (a) Isotachs in supersonic channel flow past a central body.

(b) Vorticity contours in supersonic flow past a sphere confined in a tube.

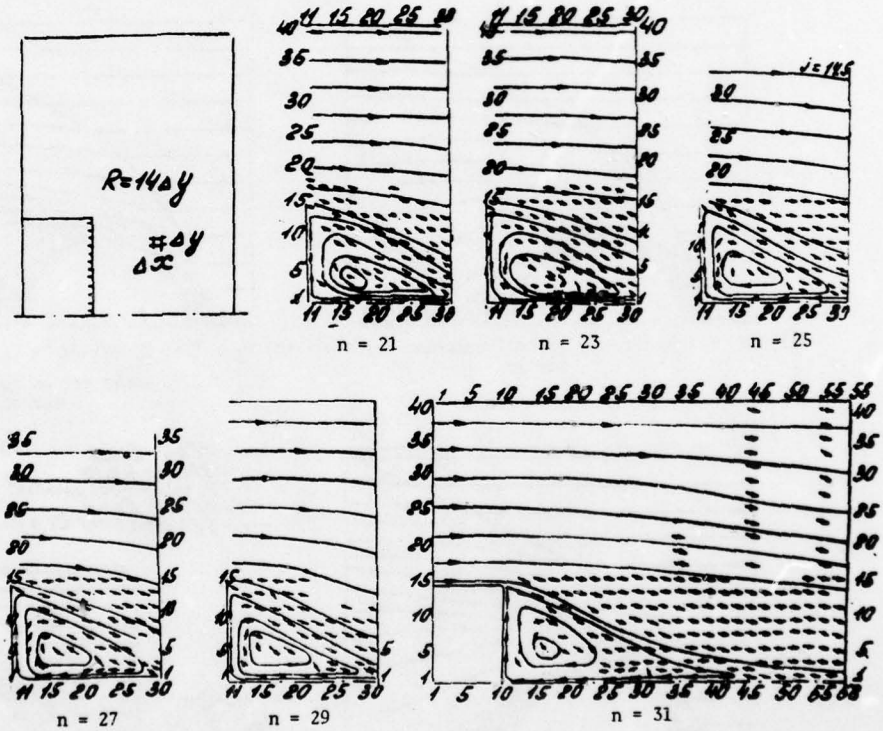

Fig. 8 Evolution of the near-base flow behind an axisymmetric cylinder with dimensionless time, n.

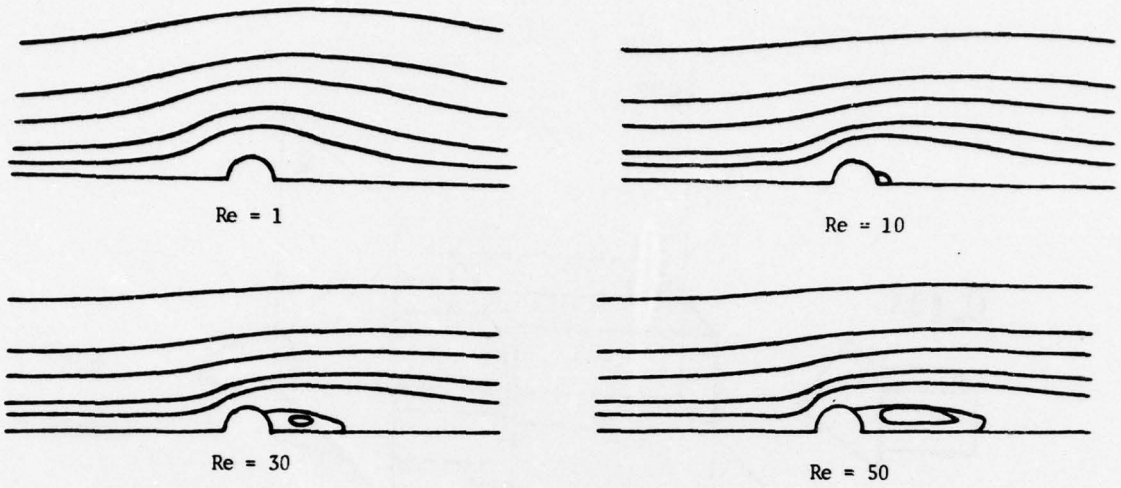

Fig. 9 Steady-state streamlines in viscous imcompressible flow past a circular cylinder.

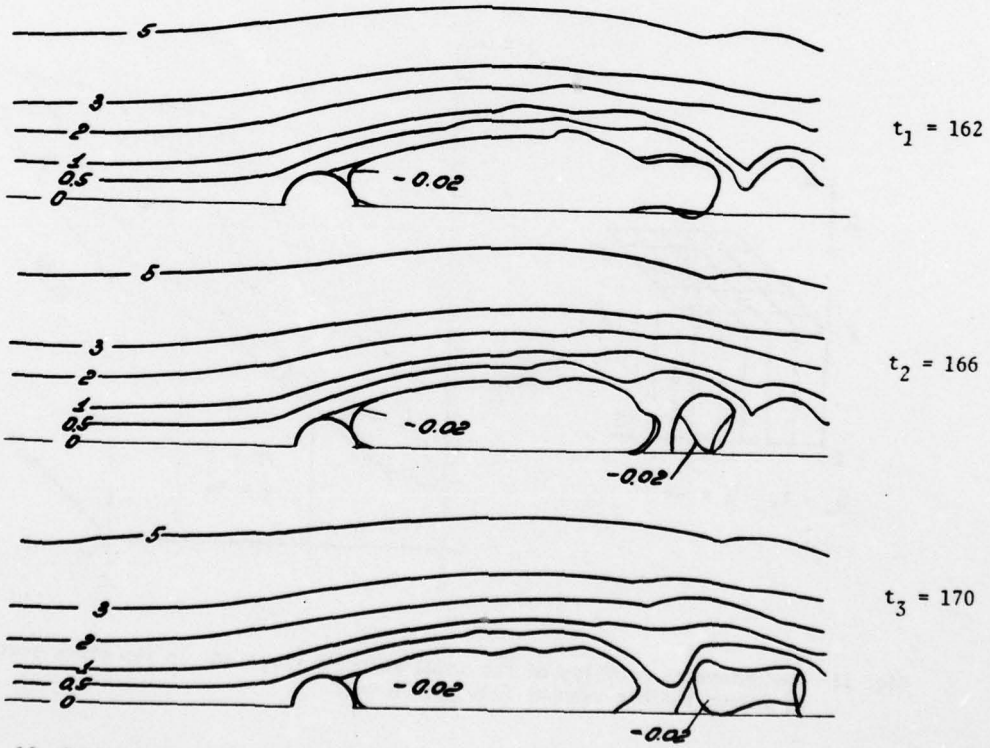

Fig. 10 Instantaneous streamline patterns in viscous incompressible flow past a circular cylinder with Reynold's number 1000.

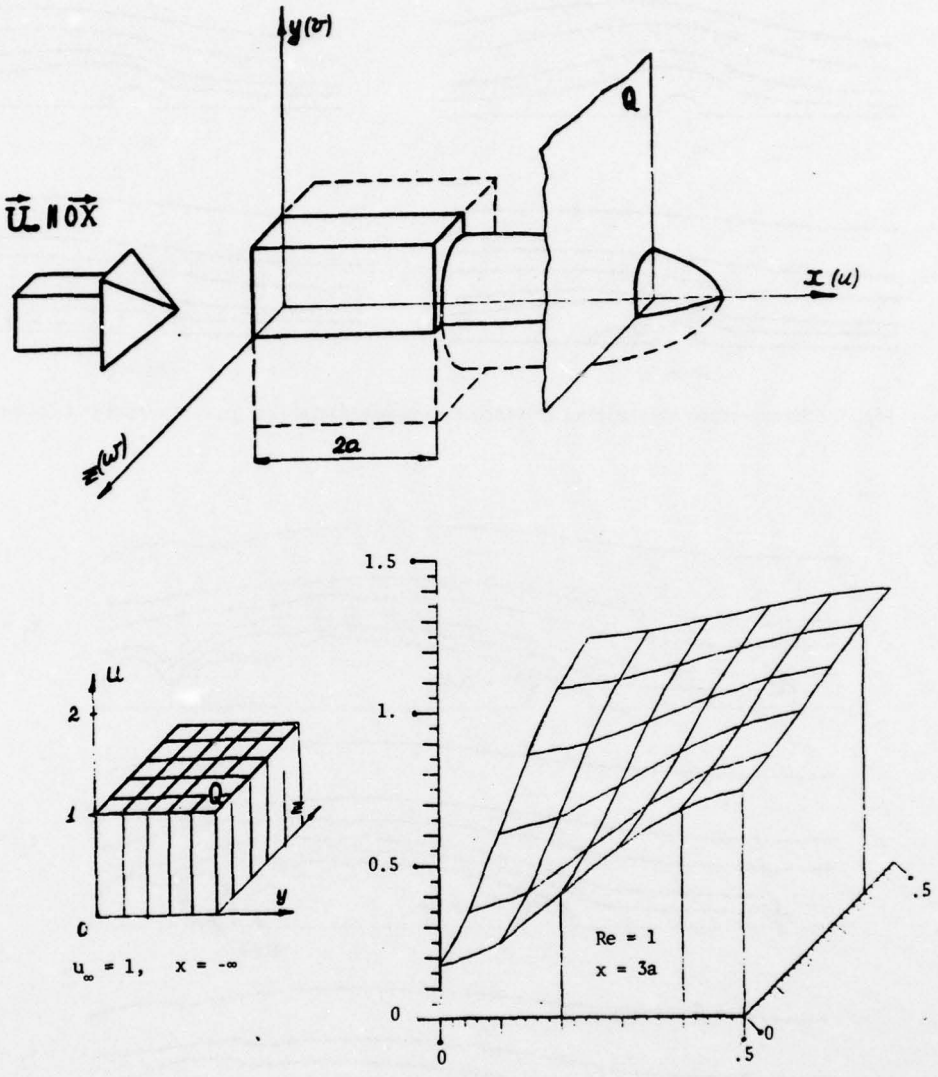

Fig. 11 Instantaneous profiles of the axial velocity component in two cross-sections of incompressible viscous flow past a cube.

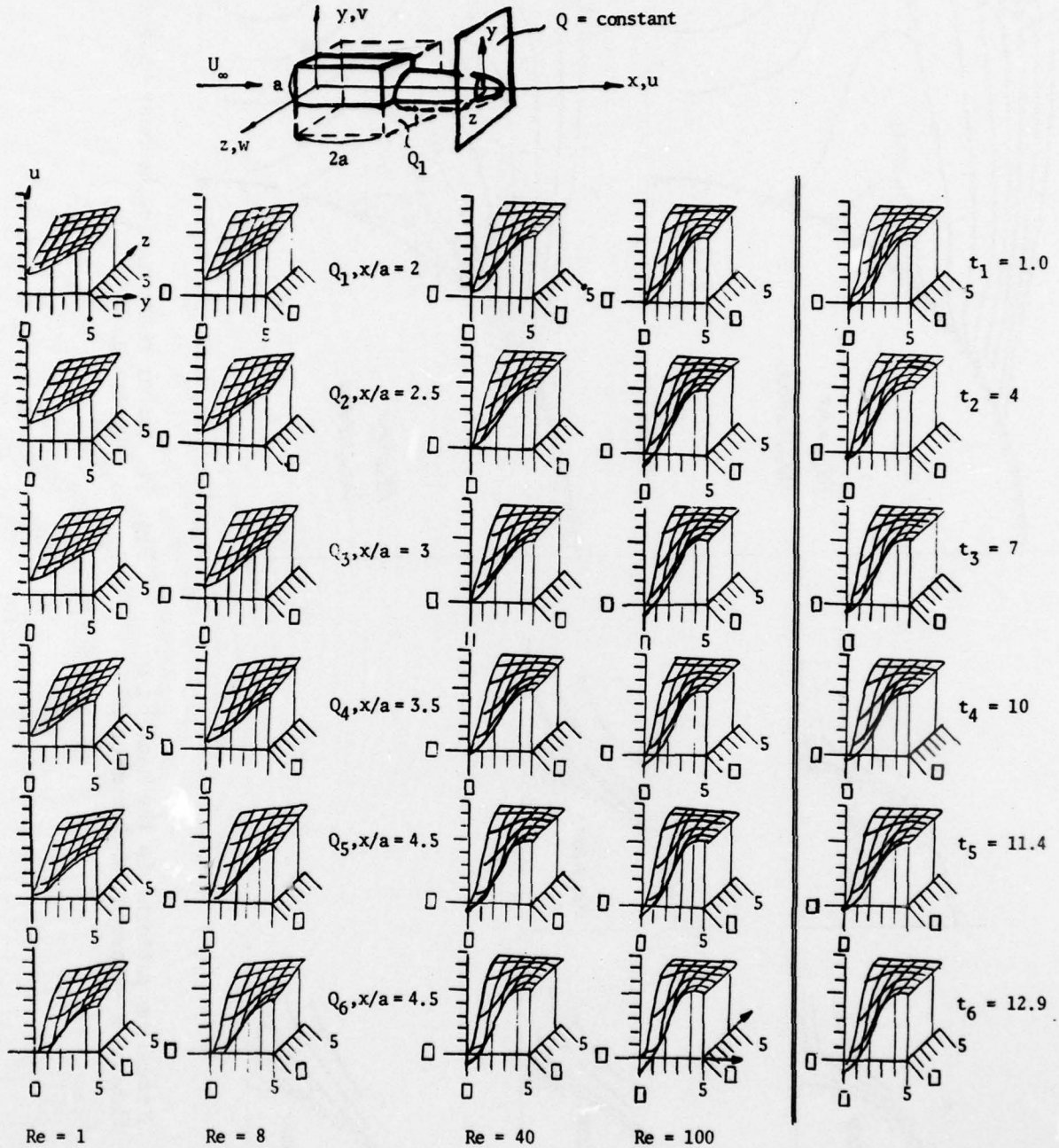

(a) Instantaneous profile of the axial velocity at various cross-sections downstream of a cube in viscous incompressible flow.

(b) Evolution with time of the axial velocity profile at the plane x/a = 4 with Re = 100.

Figure 12.

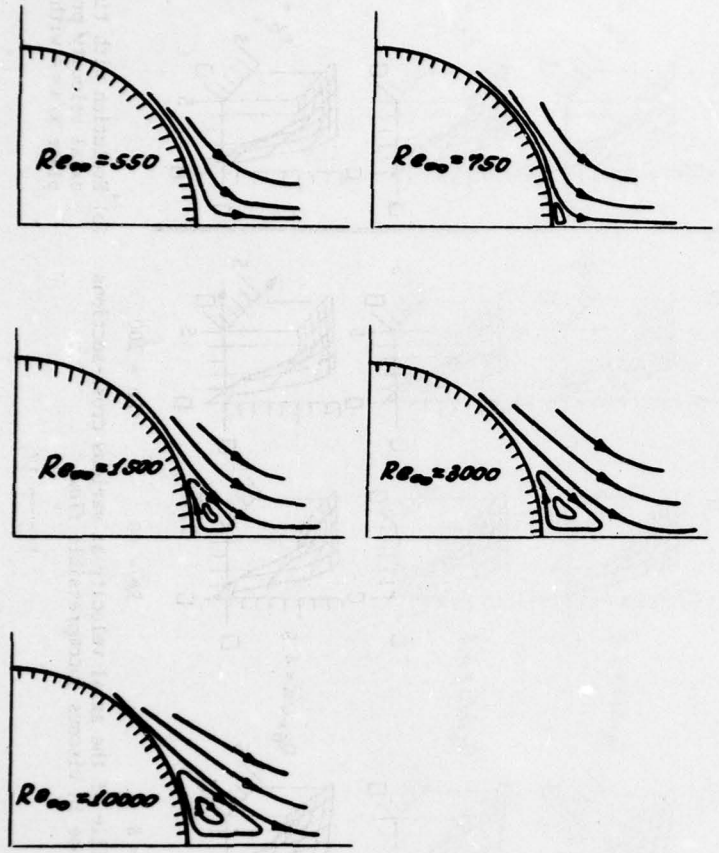

Fig. 13 Streamline patterns in the near-base flow of a sphere at Mach number 20.

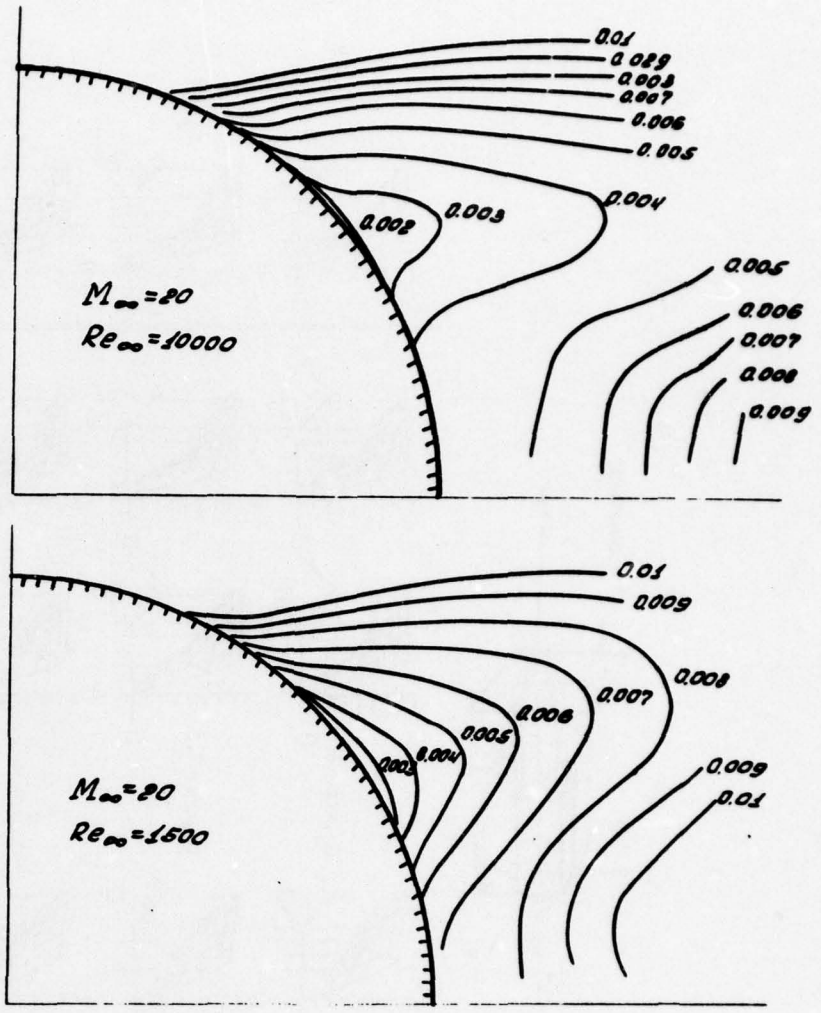

Fig. 14 Isobar contours in the near-base flow of a sphere at $M_\infty = 20$.

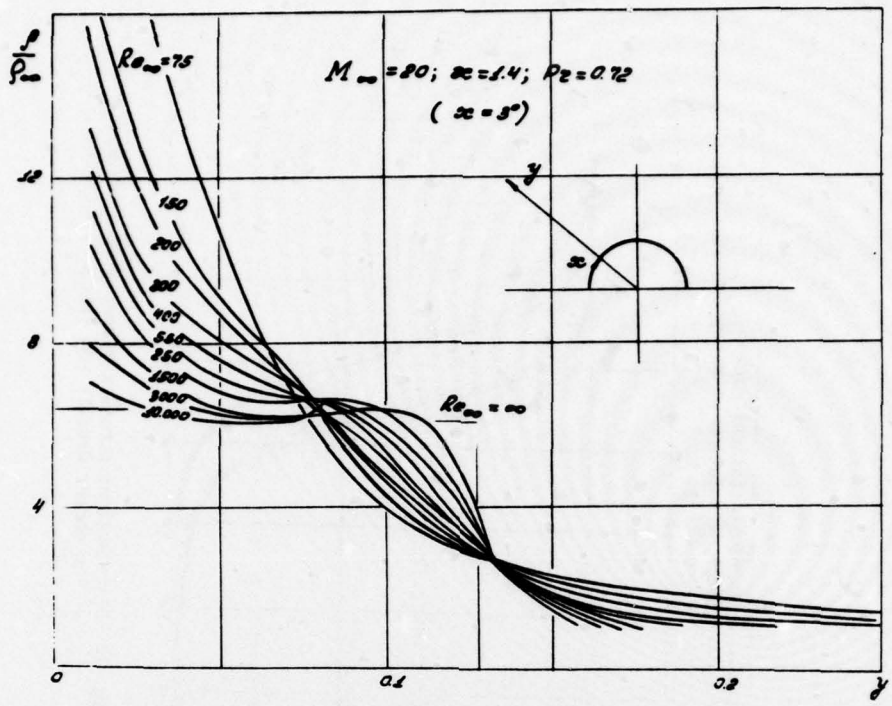

Fig. 15 Density variation across the shock layer, 3° from the stagnation point of a sphere at $M_\infty = 20$.

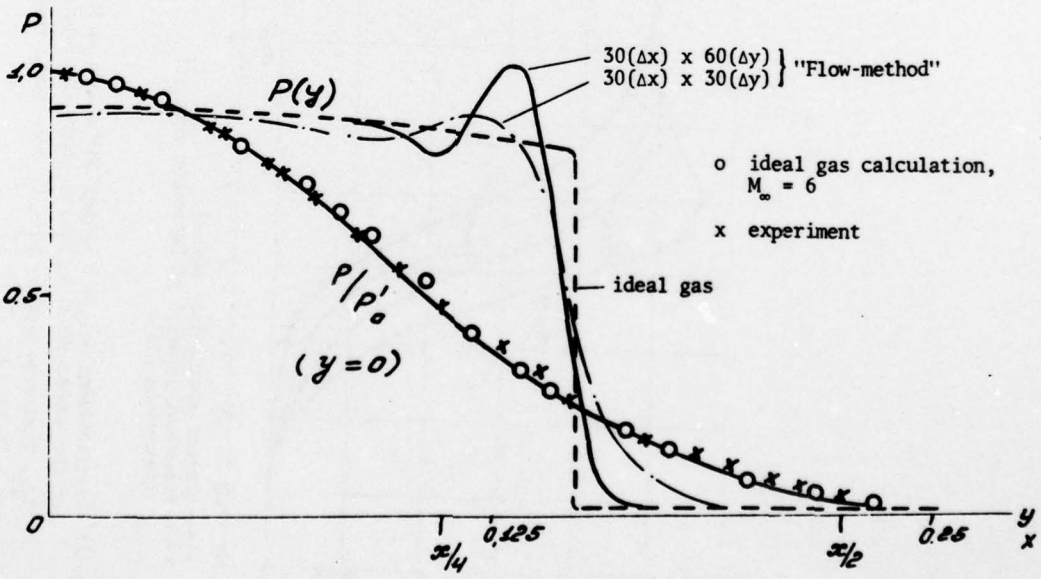

Fig. 16 Pressure distribution across the shock layer and along the surface face of a blunt body at M = 6.05 and Re = 6.43 x 10^6.

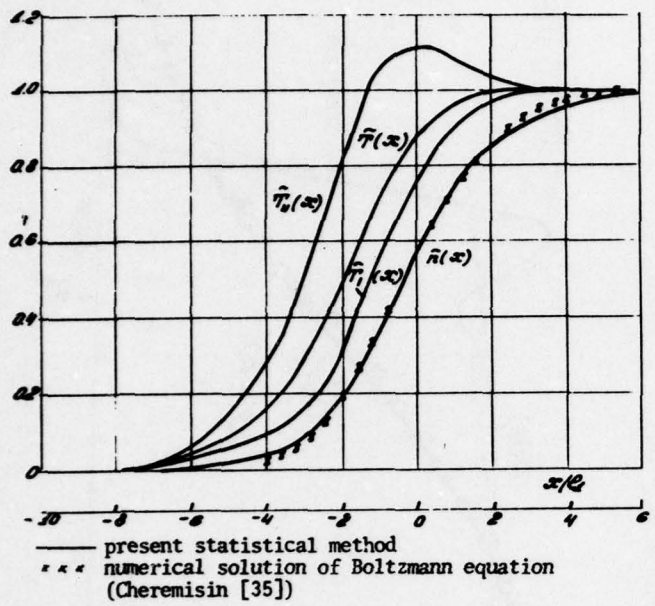

Fig. 17 Distributions across a normal shock wave at M = 2 of the number density, $\tilde{n}$, longitudinal temperature, $\tilde{T}_{11}$, tranverse temperature, $\tilde{T}_1$ and static temperature $\tilde{T}$, $15 < N_o < 20$.

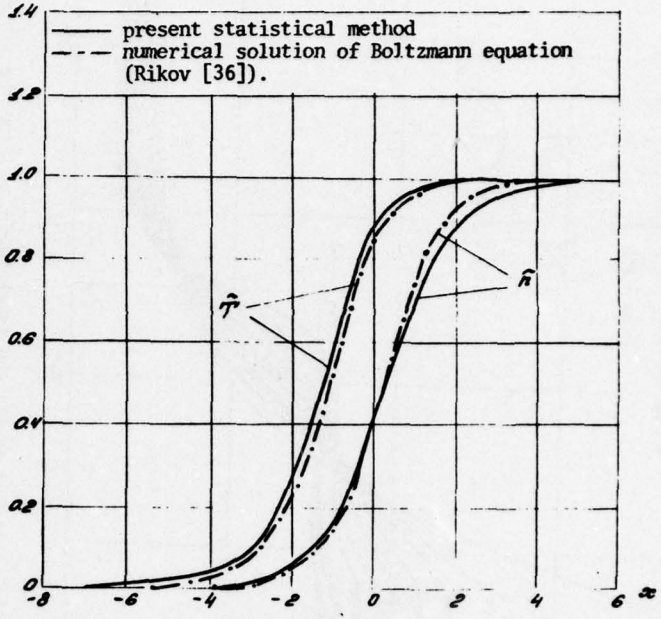

Fig. 18 Distributions across a normal shock wave at M = 3 of the number density and static temperature, $\tilde{T}$, $N_o = 12$.

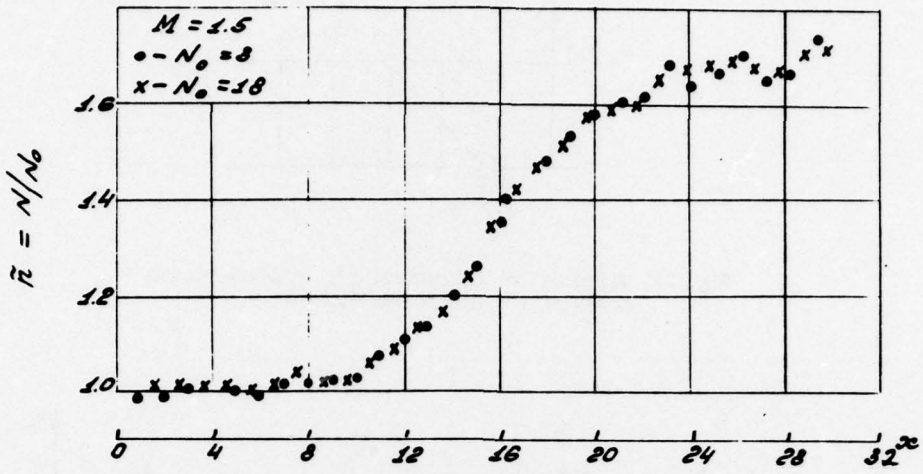

Fig. 19 Influence of the average number of particles N_o in cells on the number density distribution across a normal shock at M = 1.5.

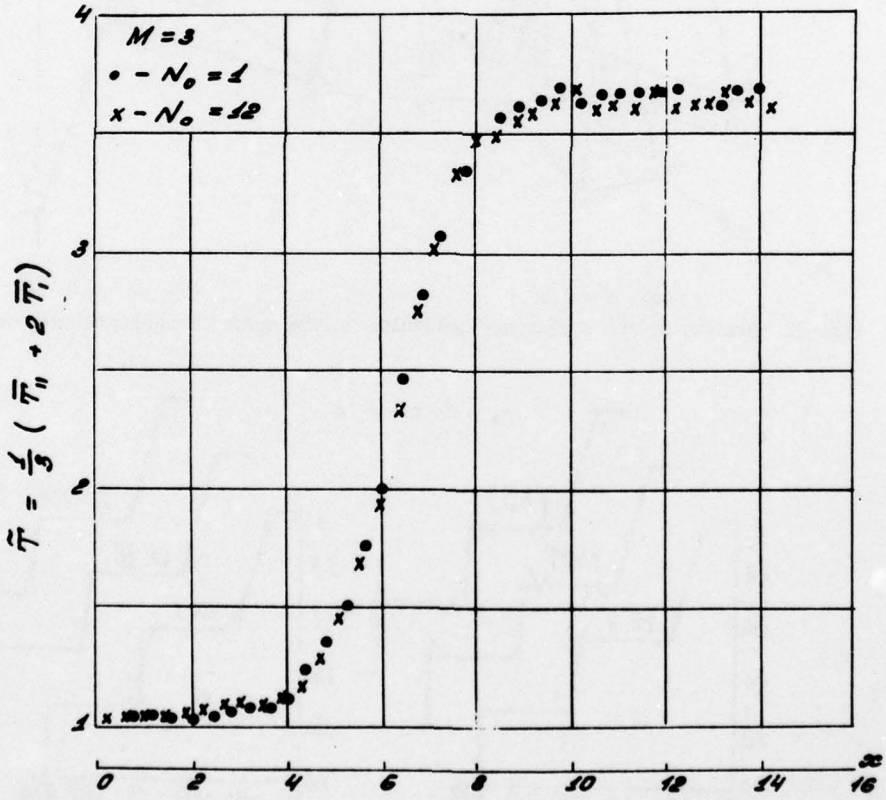

Fig. 20 Influence of the average number of particles N_o in cells on temperature distribution across a normal shock at M = 3.

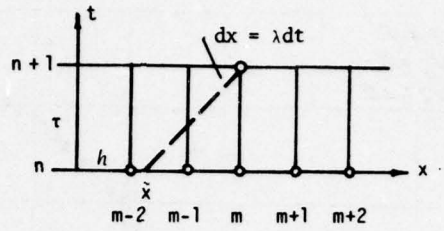

Fig. 21 Trace of the characteristic relative to the nodes of the discretization net.

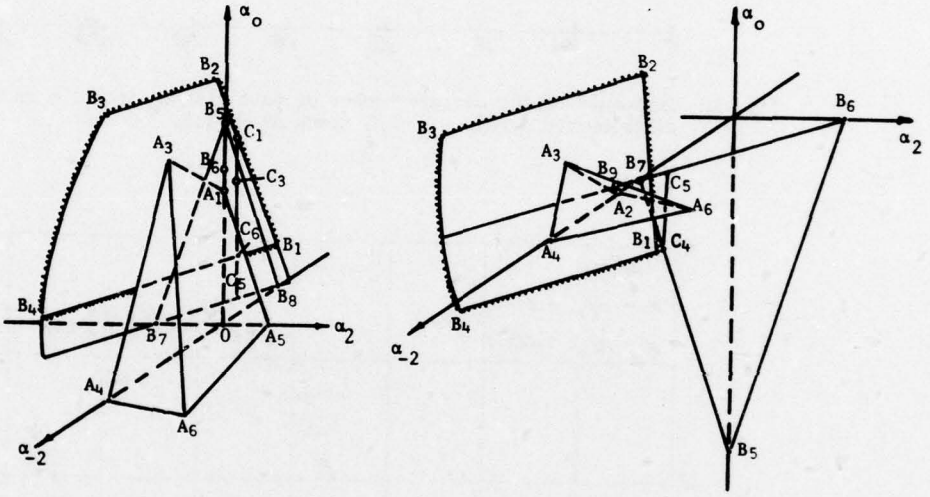

(a) σ = 0.5 (b) σ = 1.5

Fig. 22 Domains of the difference molecules in the space of indeterminate coefficients.

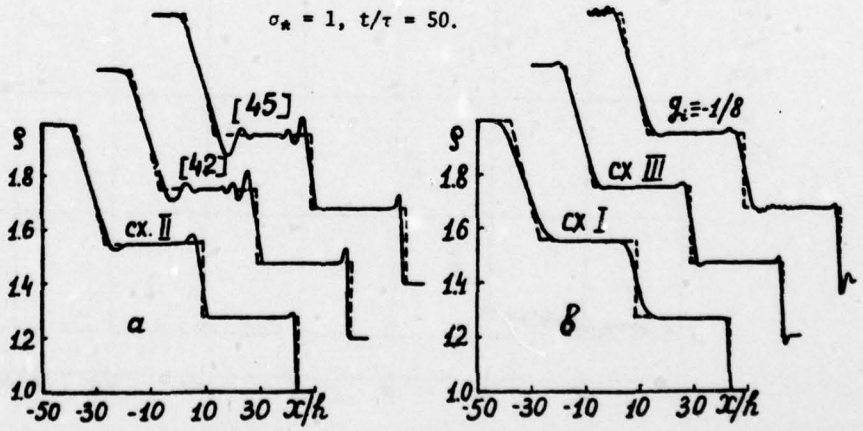

Fig. 23. Results of various difference schemes for one-dimensional wave motion in a perfect gas (---- exact solution).

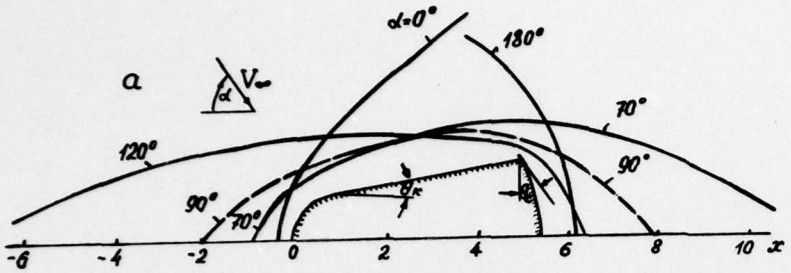

(a) Bow shock patterns in plane of symmetry of spherically-blunted truncated cone at various angles of attack with $M_\infty = 2$ and $k = 1.4$.

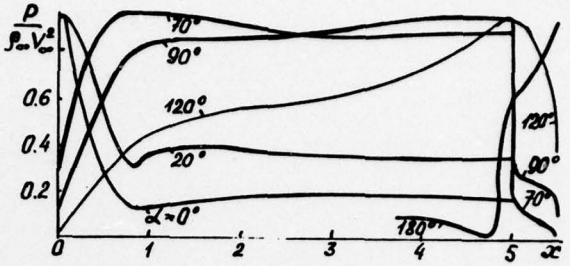

(b) Corresponding surface pressure distribution.

Fig. 24

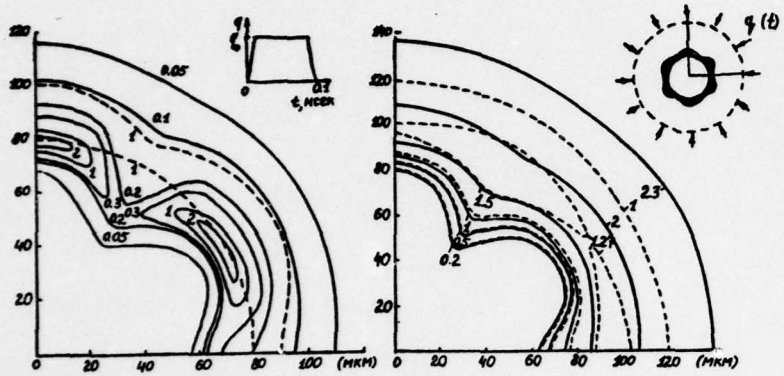

(a) (b)

Fig. 25

(a) Density field at 0.1 manosecond produced by a 300 J implosion of a pellet (--- initial inner and outer boundaries of pellet).

(b) Corresponding isotherms (Kev); —— electron temperature, --- ionic plasma temperature.

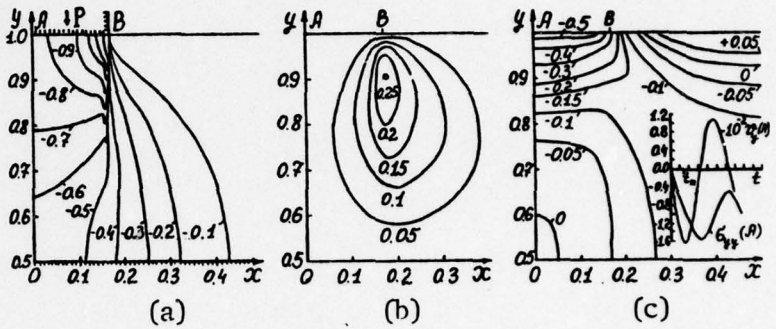

(a) (b) (c)

Fig. 26 Stress field at the instant $t = 0.029$ produced by a nonstationary loading (shown in inset (c)) of an elastic layer of unit thickness.

SECURITY CLASSIFICATION OF THIS PAGE (When Data Entered)

REPORT DOCUMENTATION PAGE		READ INSTRUCTIONS BEFORE COMPLETING FORM
1. REPORT NUMBER AE-79-1	2. GOVT ACCESSION NO.	3. RECIPIENT'S CATALOG NUMBER
4. TITLE (and Subtitle) New Computational Models in Continuum Mechanics		5. TYPE OF REPORT & PERIOD COVERED Final Technical
		6. PERFORMING ORG. REPORT NUMBER
7. AUTHOR(s) Oleg Belotserkovskii		8. CONTRACT OR GRANT NUMBER(s) N00014-79-M-0022
9. PERFORMING ORGANIZATION NAME AND ADDRESS The University of Maryland Aerospace Engineering Department College Park, Maryland 20742		10. PROGRAM ELEMENT, PROJECT, TASK AREA & WORK UNIT NUMBERS
11. CONTROLLING OFFICE NAME AND ADDRESS Department of the Navy Office of Naval Research Arlington, Virginia 22217		12. REPORT DATE March, 1979 13. NUMBER OF PAGES 83
14. MONITORING AGENCY NAME & ADDRESS(if different from Controlling Office)		15. SECURITY CLASS. (of this report) Unclassified 15a. DECLASSIFICATION/DOWNGRADING SCHEDULE

16. DISTRIBUTION STATEMENT (of this Report)

Approved for public release, distribution unlimited.

17. DISTRIBUTION STATEMENT (of the abstract entered in Block 20, if different from Report)

18. SUPPLEMENTARY NOTES

19. KEY WORDS (Continue on reverse side if necessary and identify by block number)

Computational Fluid Dynamics; Computational Modelling, Euler Solver; Navier-Stokes Equations; Boltzmann Equation; Transonic Flows; Three-Dimensional Flows; Shock Wave Structure; Hypersonic Flow.

20. ABSTRACT (Continue on reverse side if necessary and identify by block number)

Direct numerical simulation of complex gas dynamics problems (computational experiment) is performed with the help of Euler, Navier-Stokes and Boltzmann equations. The basic principles of the computational experiment are formulated and the results for various gas dynamics problems of a complex internal structure are presented.

The problems examined include the transonic regime (super-critical flows including transition through sound velocity), flows with a jet (injected → next page

DD FORM 1 JAN 73 1473 EDITION OF 1 NOV 65 IS OBSOLETE
S/N 0102-LF-014-6601

SECURITY CLASSIFICATION OF THIS PAGE (When Data Entered)

Block number 20 continued.

into the main stream and diffraction problems. Body wake flows are studied at various Reynolds numbers. The structure of a shock wave provides an example of rarefied gas flows at various Mach numbers.

A set of control tests is worked out for the estimation of calculation accuracy.